

## The effects of seasonal variations in rainfall and production on the aquifer and surface features of Rotorua geothermal field



Thomas M.P. Ratouis<sup>a,\*</sup>, Michael J. O'Sullivan<sup>a</sup>, Samantha A. Alcaraz<sup>b</sup>, John P. O'Sullivan<sup>a</sup>

<sup>a</sup> Department of Engineering Science, The University of Auckland, Auckland 1142, New Zealand

<sup>b</sup> GNS Science, Private Bag 2000, Taupo 3352, New Zealand

### ARTICLE INFO

#### Keywords:

Geothermal modelling  
Rotorua geothermal field  
Monitoring programme  
Resource management

### ABSTRACT

The Rotorua geothermal field is a shallow geothermal reservoir lying directly beneath Rotorua City in New Zealand. It is renowned for an abundance of natural geothermal manifestations including the geysers and hot springs at Whakarewarewa. Over-exploitation of the geothermal resource in the 1970s leading to the decline of many active surface features was recognised and subsequently addressed by a change of management policy. A wellbore closure programme was instigated in 1986 by the New Zealand government which resulted in the recovery of some of the geothermal features. The monitoring programme continues through to the present day and provides valuable data which is used for the calibration of the new numerical model of the Rotorua system presented here. This model focuses on seasonal factors that control water level fluctuations in the geothermal reservoir as well as the behaviour of individual surface features. The matches of model temperatures with field data from individual surface features are very promising and the model may assist with sustainable management of the geothermal resource.

### 1. Introduction

The Rotorua geothermal field (RGF) is a geothermal reservoir which lies beneath Rotorua City in the Taupo Volcanic Zone (TVZ) located in the North Island of New Zealand (Fig. 1). It is renowned for an abundance of natural geothermal manifestations and contains one of New Zealand's last remaining areas of major geyser activity at Whakarewarewa (Fig. 1). In total, 1570 geothermal features have been identified and referenced in the RGF (Graham et al., 2013; Fig. 2).

However close proximity of the resource to a population centre and ease of access for end-users resulted in intensive drilling and fluid abstraction from shallow bores for domestic and commercial usage from the 1950s onwards. This led to a decline of springs and geyser activity in the 1970s. Increasing concern about the effect of geothermal fluid withdrawal on the geothermal surface activity led to the establishment of the Rotorua Geothermal Monitoring Programme (RGMP) in 1982 (O'Shaughnessy, 2000). Monitoring bores (M-wells) and shallow monitoring bores (G-bores) were drilled throughout Rotorua City and have been used to record water levels and temperatures in the geothermal aquifer as part of the RGMP (Fig. 1). By 1986, aquifer pressures declined to the lowest levels since the monitoring programme began (Bradford, 1992) and to prevent further deterioration of spring and geyser activity a Bore Closure Programme was enforced (Gordon et al.,

2005).

By 1988, the programme contributed to a 75% decrease in net withdrawal (Bradford, 1992) and an immediate increase in reservoir pressures was observed (Fig. 16). During the ensuing years recovery of some surface features was also observed (Scott et al., 2005). In 1991 Environment Bay of Plenty (EBOP) assumed responsibility for managing the field under the Resource Management Act to "monitor the recovery of geothermal features and protect the surface manifestations while providing allocation of the resource for present and future efficient use" (EBOP, 1999). As part of the new management regime, forty-one of the most significant features were selected for further observation and have been monitored on a monthly basis since May 2008 (Fig. 2). Along with the network of Monitoring Wells, these data provide valuable information on the state of the reservoir and the activity of geothermal surface features and may help to distinguish the impact of variations in the natural recharge from that of changes in production strategies.

To support the management plan of the geothermal resource, detailed numerical models of the RGF have been developed at the University of Auckland. These models have been gradually refined and improved from a coarse air-water model (UOA Model 1–2) (Febrianto et al., 2013), (UOA Model 3) (Ratouis et al., 2014) to a finer air-water model (UOA Model 4) (Ratouis et al., 2015), and to a chloride and

\* Corresponding author.

E-mail address: [t.ratouis@auckland.ac.nz](mailto:t.ratouis@auckland.ac.nz) (T.M.P. Ratouis).

## North Island, New Zealand

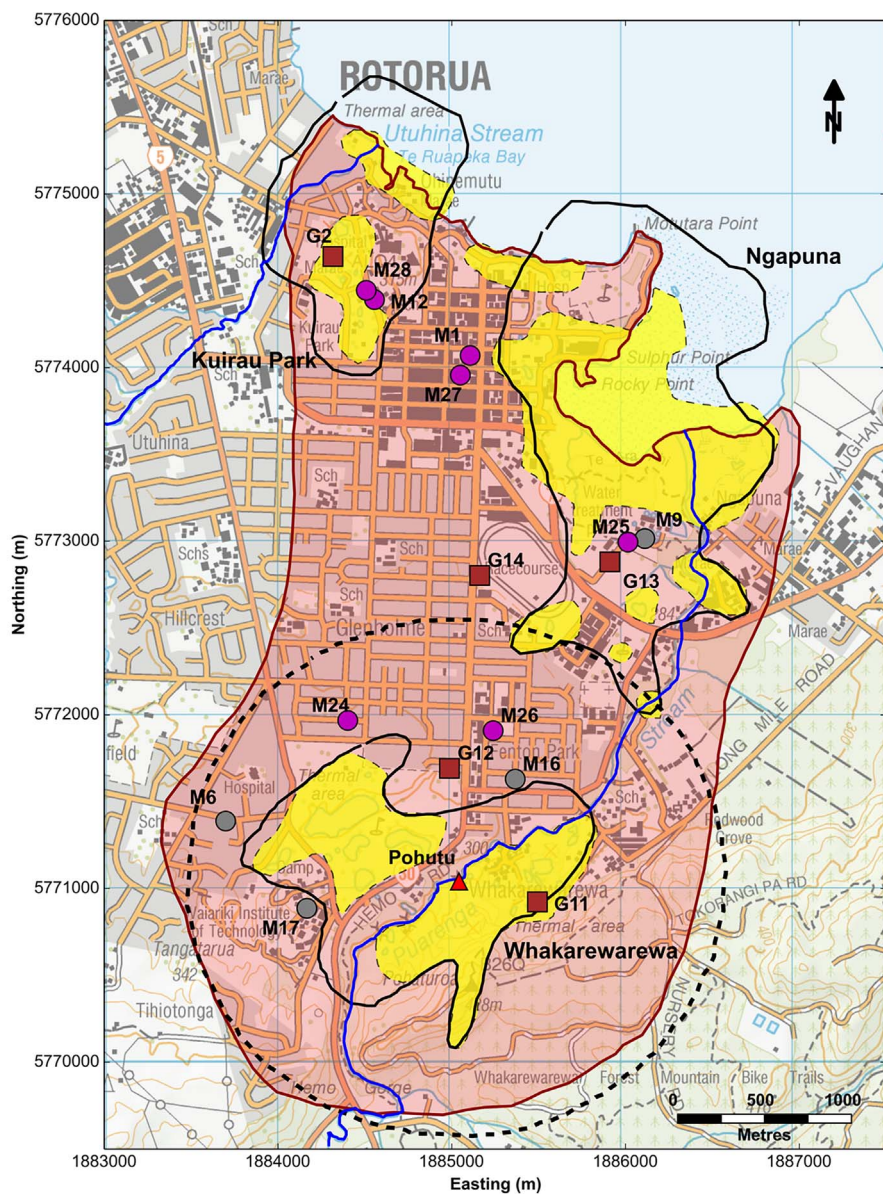
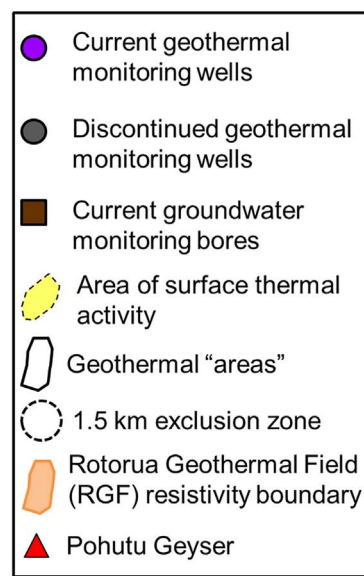
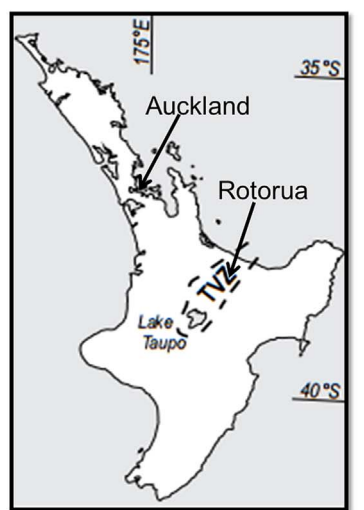


Fig. 1. Map of the Rotorua Geothermal Field showing the extent of the field, areas of surface activity, and locations of monitoring wells.

carbon dioxide model (UOA Model 4a) (Ratouis et al., 2016a).

UOA Model 5 presented in this paper is an extension of UOA Model 4a (Ratouis et al., 2016a) and includes a number of modifications to represent more realistically the geothermal field and to improve the match to aquifer pressures and the behaviour of individual surface features (temperatures, mass flows and pressures). The changes to the model include the following:

- More accurate allocation of production and reinjection to individual well users,
- Inclusion of seasonal rainfall and seasonal production and reinjection rates,
- Re-evaluation of the downhole and surface temperatures,
- Refinement of the permeability structure based on the new temperature distribution, and
- Further model calibration to match the updated temperature contours and the temperatures of the surface features.

In the work presented here an emphasis is placed on the variations in rainfall and anthropogenic fluid extraction, both of which could have

a large impact on the geothermal reservoir water levels and surface activity. The aim is to complement and to help interpret the Rotorua monitoring programme data by providing a tool which can identify spatial and temporal trends of both natural and anthropogenic disturbances. It is hoped that the model can then be used to distinguish naturally occurring disturbances from man-made effects on reservoir pressures and the activity of geothermal surface features. Then it can be used to evaluate any beneficial or adverse impact on surface features associated with the current or future allocation of the geothermal resource.

## 2. Natural disturbances effecting the rotorua geothermal field

The generic effects of natural disturbances on a geothermal reservoir and surface features, common to all geothermal fields, are discussed in this section as well as some effects special to Rotorua. These diverse factors can impact the behaviour of the geothermal systems over various timescale; some will affect reservoir pressures and surface features activity immediately (changes in barometric pressure) while other might take hundreds of years (deep meteoritic recharge of the

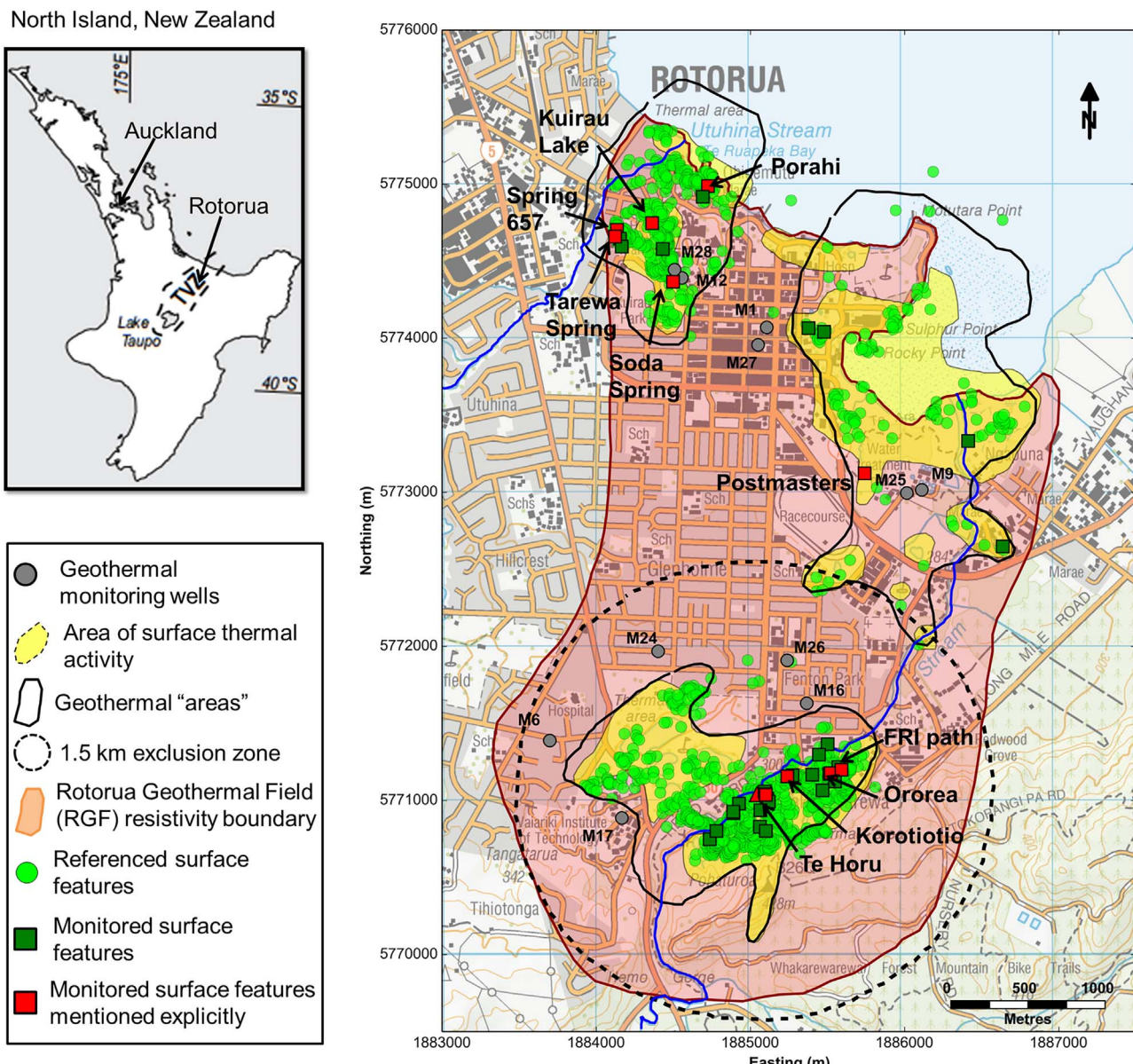


**Fig. 2.** Map of Rotorua City showing the locations of geothermal features referenced by GNS Science (lime circle) and features currently monitored as part of the Rotorua monitoring programme (green square). Surface features mentioned explicitly in this paper are represented in red. (For interpretation of the references to colour in this figure legend, the reader is referred to the web version of this article.)

geothermal fluid).

### *2.1. Supply of geothermal fluid*

The supply of geothermal water to the shallow reservoir at Rotorua originates from deep in the geothermal system and flows through a network of faults and fractures to the surface (Wood, 1992). For the Rotorua system the predominant constituent of the deep geothermal fluid is meteoric water – estimated at 83% – with a small portion of arc-type magmatic water (Giggenbach, 1995). This implies a convective circulation of meteoric water that percolates from the surface to the deeper part of the TVZ where it is heated by a silicic magma intrusion (Heise et al., 2015). This induces a buoyancy-driven upflow along the southern edge of the Rotorua Caldera. Therefore changes in the heat source, strain rates or effective stresses of the faults supplying the geothermal fluid (Kissling et al., 2009) as well as long term rainfall trends can impact the supply of high-enthalpy geothermal water. In Rotorua, temperatures in monitoring wells (M9 and M16) have

remained almost constant throughout the monitoring campaign in Ngapuna and Whakarewarewa (Fig. 1) (Kissling, 2014) indicating little change in the geothermal fluid supply at depth. The total natural deep upflow of the Rotorua system has been estimated by Scott and Cody (1997) to be approximately 77,500 t per day. The inflow of hot water injected at the bottom of the model to represent the natural deep upflow is assumed to be constant throughout the simulations (Table 2).

## 2.2. Barometric pressure

The barometric pressure or atmospheric pressure is influenced by elevation, the level of cyclonic activity, surface temperature, and solar radiation (Bluestein, 1993). Water table levels react instantaneously to imposed barometric pressure changes (Weeks, 1979) which in turn may affect the filling and/or heating rates of geysers and springs and hence the surface activity of geothermal features (Nikrou et al., 2013). However the current model does not have the temporal and spatial resolution required to model the cyclic behaviour of individual geysers

and springs. Barometric pressure changes are also transmitted down the geothermal bores to the geothermal aquifers but these fluctuations are not representative of the conditions in geothermal reservoir. The water level response to barometric changes seen in the geothermal monitor wells is therefore considered as noise (Bradford, 1992). For these reasons, changes in atmospheric pressure are not included and pressures from monitoring wells are corrected for barometric pressures.

### 2.3. Earth tides

Periodic changes in the solid structure of the Earth due to earth tides cause changes in the pressures of subsurface fluids (Leaver, 2006). The amplitude of the response to earth tides is dependent on the regional geology, crustal geometry, regional strain field and ocean loading (Arditty and Ramey, 1978; Hsieh et al., 1988) while the response of water levels in aquifers to earth tides is dependent on the period of the disturbance, and permeability of the formation (Narasimhan et al., 1984). Leaver performed a wavelet and Fourier analysis of hourly pressure changes in Monitoring well M6 (Fig. 1) from July 1996 to 30 June 1998 (Leaver, 2006). He found that the effect of Earth tides on variations in water level were not significant and were an order of magnitude less than effects due to other factors. Therefore earth tides have not been included in this study.

### 2.4. Lake Rotorua levels

Variation of the level of Lake Rotorua modifies the pressure applied at the bottom of the lake and thus affects the amount of water flowing into or out of the bottom of the lake. However lake levels have been stable for many years (Bay of Plenty Regional Council, 2017) Bay of Plenty Regional Council, Lake Rotorua Water Level) and are set to be constant at 280 masl in the model.

### 2.5. Temperature of Lake Rotorua and the ambient temperature

No direct correlation between the temperature of Lake Rotorua or the air temperature with surface feature activity has been observed (Nikrou et al., 2013). In the model the lake temperature is set at 10 °C and the air temperature is fixed at 15 °C.

### 2.6. Rainfall and urbanisation changes

The amount of water supplied to the shallow ground water from rainfall is controlled by the infiltration rate which is the difference between the amount of rainfall that permeates to the water table and the amount lost to surface runoff. Short-term changes in the rainfall pattern affect the amount of water supplied to the shallow ground water and cause changes in the chemical and thermal composition of geothermal springs as well as causing pressure fluctuations (Leaver, 2006). Longer term changes in mean rainfall affect the deep groundwater storage and mixing with the high-enthalpy geothermal fluid (Bradford, 1992).

Mean rainfall in Rotorua has been variable throughout the 20th century. It was high during the 1960s and early 1970s and then declined in the early 1980s after which it stabilised at a lower level (Fig. 3). Bradford (1992) investigated long-term rainfall changes and concluded that about half of the pressure drop in the production aquifers may have resulted from a decline in rainfall, together with the increasing urbanisation of Rotorua City and the consequent diversion of runoff waters and sub-surface drainage. Monthly-averaged rainfall with a background infiltration rate of 10% and an “urban zone” limited infiltration rate (8%) were included in the model.

## 3. The effect of anthropogenic disturbances on the Rotorua geothermal field

### 3.1. Impact on the geothermal reservoir and surface activity

Exploitation of the geothermal waters in Rotorua increased steadily and geothermal bores proliferated from 1950 onwards, peaking at about 400 bores in use, drawing some 31,000 t per day in the winter of 1985 (Ministry of Energy, 1985). The winter drawoff in 1985 accounted for approximately 40% of the total outflow from the geothermal field and was almost double the natural flow from Whakarewarewa of approximately 17,000 t per day (Ministry of Energy, 1985). Nearly all of the thermal water was drawn from aquifers in the top of either the Rotorua Rhyolite or the Mamaku Ignimbrite (Wood, 1992) and disposed of at the surface via shallow “soak bores” (usually between 10 and 20 m deep) or to surface watercourses (Gordon et al., 2005). The intensive exploitation phase of the geothermal resource at Rotorua was accompanied by an increasing number of failures of geysers and springs.

For example:

- The Tarewa Springs became dormant during the 1950s-1970s,
- Kuirau Lake stopped overflowing in the 1970s,
- Waikite Geyser stopped erupting in 1967,
- Kereru Geyser stopped erupting in 1972,
- Te Horu Geyser experienced a decline in eruption frequency in 1972 and stopped overflowing in 1987,
- Papakura geyser last erupted in 1979, and
- There was a decline in the frequency, duration and character of eruptions of Pohutu geyser from 1982 (Cody and Lumb, 1992).

However, up to the early 1980s, little information was available on the natural state of the surface activity and estimation of potential anthropogenic-induced changes in springs and geyser activity was difficult, given the high natural variability in the activity of thermal features. Thus it was difficult to demonstrate at the time that the drawoff through the many shallow bores in the field was the actual cause of decline in reservoir pressures and surface activity. As a consequence the central government and Ministry of Energy initiated in 1982 the Rotorua Geothermal Monitoring Programme (RGMP) (O'Shaughnessy, 2000). Geothermal Monitor Wells (M1, M6, M9, M12 and, M16) were drilled throughout Rotorua city to monitor the pressure levels within the rhyolite and ignimbrite geothermal aquifers (Fig. 1).

They showed that, by 1985, as winter production rates peaked, aquifer pressures declined to the lowest levels observed since the start of the monitoring programme in 1982 (Bradford, 1992). Well owners were known to regulate their production according to need and so more water was withdrawn during the winter (Boreham, 1985). Moreover fluctuations in water levels in monitoring wells from 1982 to 1987 showed a seasonal cycle with low pressures during the winter months (Fig. 17). Furthermore, Grant (1986) noted that a seasonal pattern was also observed in the springs: “In recent years there have been a number of temporary and permanent spring failures. These all occur over autumn-winter, i.e. the time of low aquifer pressure and high groundwater pressure. (...) Roto-A-Tamahere, the largest spring, is now instrumented and appears to show a winter drop of 10–15% in flow, based on the part-year record available.” The effect of drawoff on the surface features was also highlighted by Bradford (1992). She noted that in the mid-1980s the difference between summer and winter mass withdrawal was accompanied by a rise in pressure in the aquifer of about 0.07 bar in summer months and that the natural activity of several springs increased during the same period which could “not be related to climatic changes and were likely related to the seasonal variation in aquifer pressure” (Cody and Lumb, 1992).

These observations led the scientists involved with the RGMP to conclude that changes in reservoir pressures were caused by utility

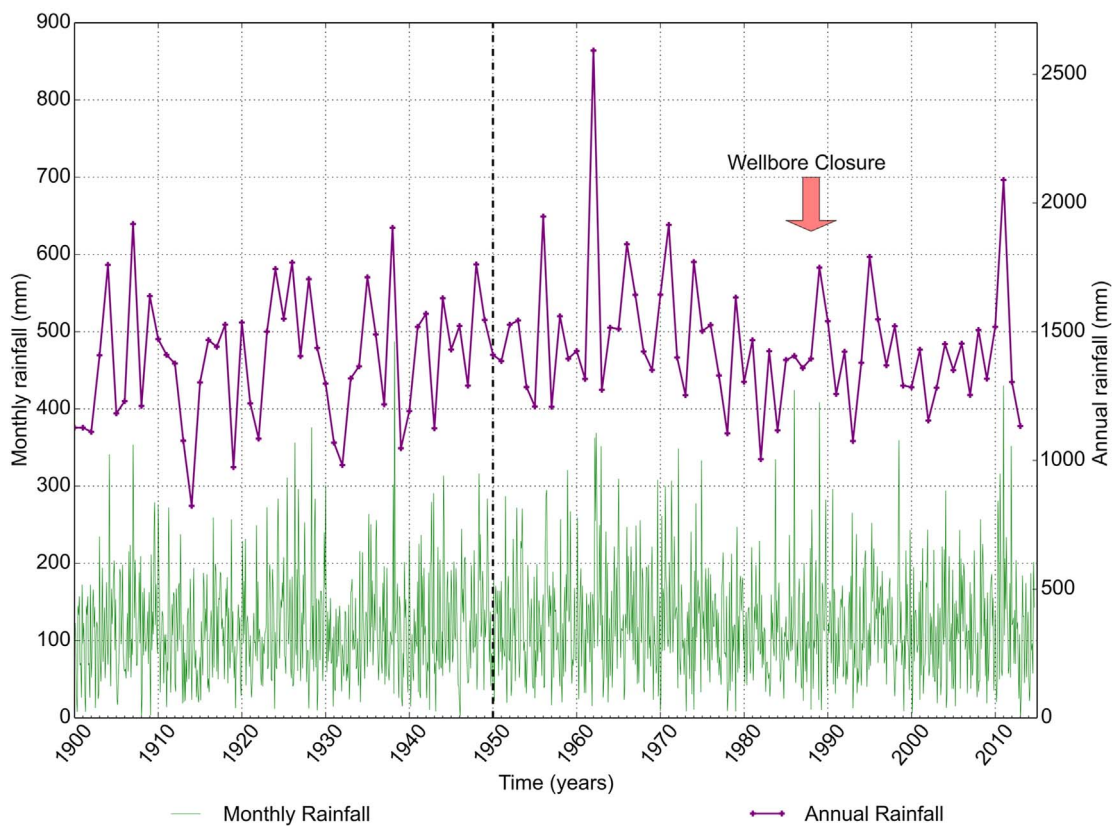


**Fig. 3.** Annual and monthly-average rainfall in Rotorua from 1950 to 2014 collected at Kaituna at Whakarewarewa by Environment Bay of Plenty.

drawoff and that production from shallow geothermal wellbores in the RGF had an adverse impact on the springs and geyser activity. They advised that urgent action was required to prevent further deterioration.

This resulted in the introduction of a Wellbore Closure Programme in 1986 which involved:

- Closure of all bores within a 1.5 km radius of Pohutu Geyser (Whakarewarewa),
- Closure of all government-owned wells in Rotorua township,
- Implementation of a charging regime for extracting geothermal fluid and
- Reinjection of waster geothermal fluid into the reservoir rather than discharge into surface watercourse and via shallow soakage (Gordon et al., 2005).

The Wellbore Closure Programme resulted in an overall reduction in the number of extraction sites because a large number of domestic bores were grouted in response to the imposition of the resource rental regime (Gordon et al., 2005; Fig. 4). The number of reinjection bores has progressively increased due to the requirement in the Rotorua Geothermal Regional Plan for full reinjection (Fig. 4). Reinjection at Rotorua is a corner stone of the management policies of the Plan; work undertaken during the formulation of the Plan indicated that conservation of mass within the Field was the key to maintenance of geothermal aquifer water levels, and by association, continued activity of geysers, springs and other surface outflow features.

By 1988, the programme resulted in a 66% reduction in production (10,830 t per day) and a 75% decrease in net withdrawal (7150 t per day) (Bradford, 1992). It was followed by a rapid increase in pressure (0.1–0.2 bar; Fig. 16) and recovery of some surface features during the ensuing years was observed:

- The Tarewa springs resumed boiling and overflowing in 1988,
- Kuirau Lake resumed overflowing in 1989,
- Te Horu Geyser resumed overflowing in 2000,
- Eruptions of Kereru recommenced in 1988 (but remain rare to this day), and
- Papakura resumed boiling in September 2013 and first erupted in September 2015

These observations highlight that unregulated mass extraction negatively impacted surface activity at Rotorua and that a regulated extraction scheme with pressure support from in-reservoir reinjection has had a positive impact on the system. The recovery of the Rotorua geothermal field was more widely discussed in Scott et al., 2005 and readers are referred to this paper for additional information.

### 3.2. Production estimates

Annual production and reinjection rates for the RGF from 1950 to 2005 have been estimated by the RGMP and EBOP (RGMP, 1985; Gordon et al., 2005) and are shown in Fig. 5. These estimates were extended by the authors to 2015 using current geothermal extraction consents for the RGF provided by EBOP (Rotorua Geothermal Current Consents – 20141104).

Disposal of used geothermal fluid into shallow soak bores and surface watercourses prior to 1986 is currently not included in the model due to lack of official records, estimates of the mass reinjected, and information on flow pathways (i.e. the proportion of waste geothermal fluid which fed directly into streams and Lake Rotorua is not known therefore the waste water recharge into the geothermal reservoir is uncertain).

In previous models of the RGF, the estimated production rate was distributed uniformly across all the wells for which temperature data were available and wells within the 1.5 km exclusion zone around

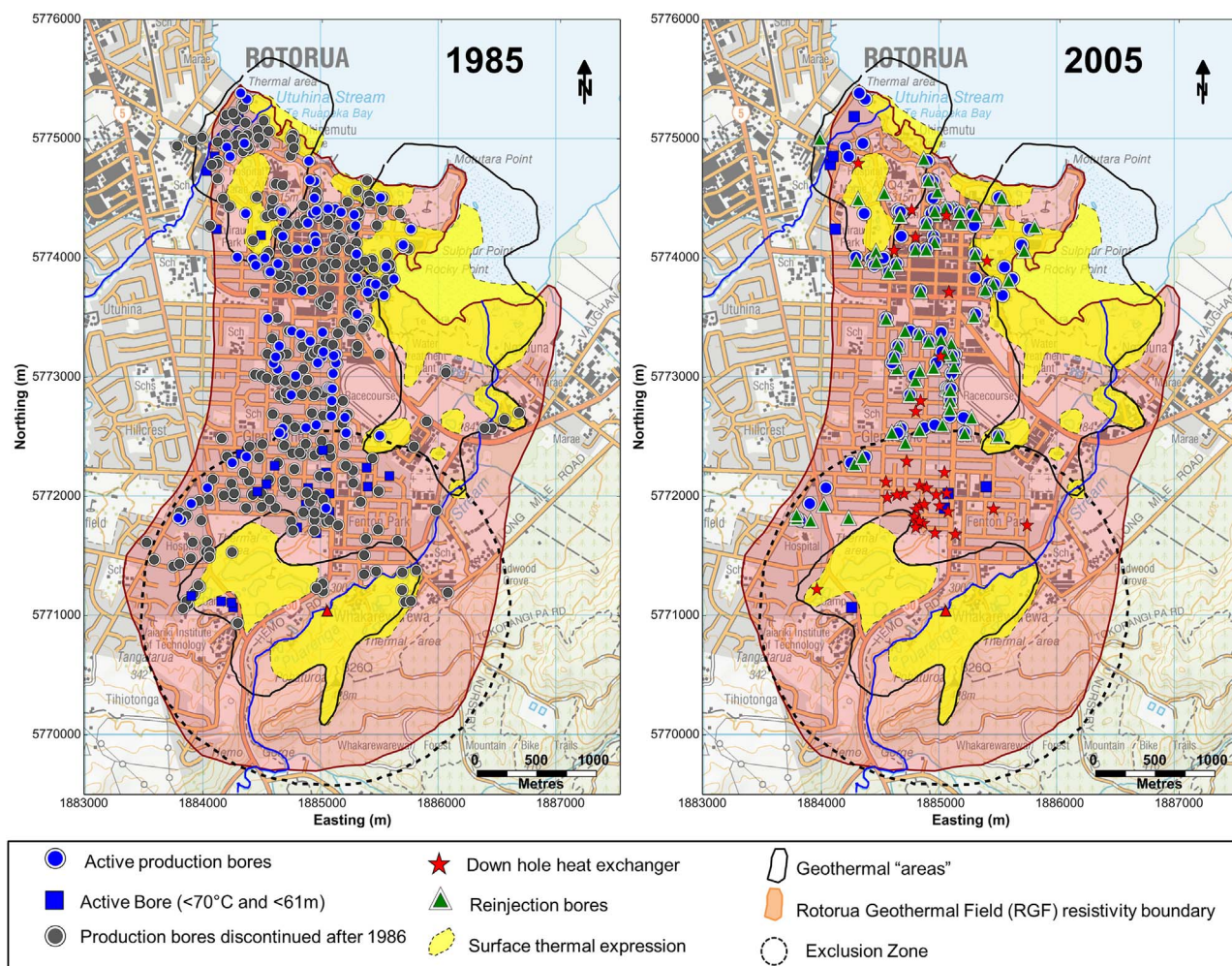


Fig. 4. Distribution of geothermal wells in Rotorua City before the Bore Closure Programme (left) and in 2005 (right).

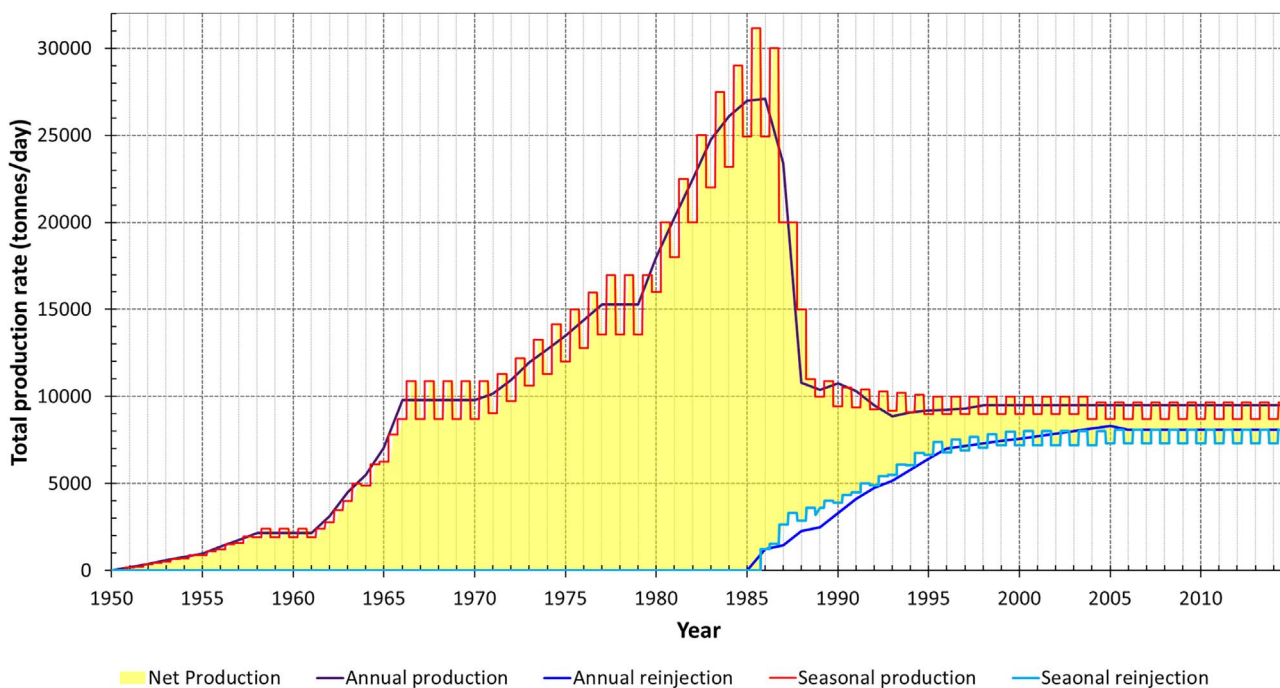


Fig. 5. Annual and seasonal mass production and reinjection estimates for the RGF from 1950 to 2015.

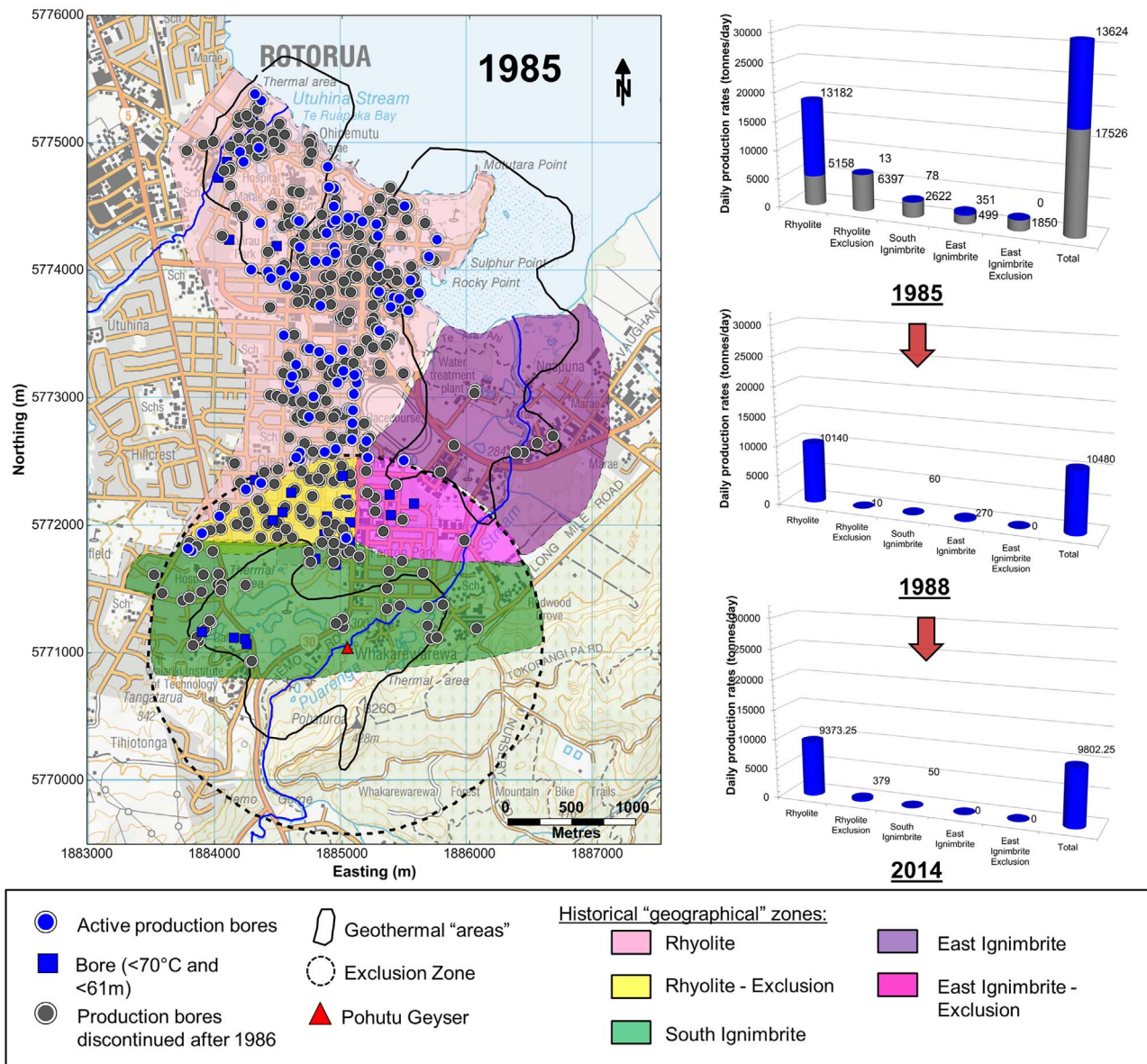


Fig. 6. Five geographical zones defined by Bradford (1992) and production rates for current (blue) and old wells (grey) in 1985, 1988, and 2014 per geographical zones. (For interpretation of the references to colour in this figure legend, the reader is referred to the web version of this article.)

Pohutu Geyser were shut after 1986 (Ratouis et al., 2016a). For the current model, an assessment of the production and reinjection at individual wells was undertaken. Two types of wells are discussed: current and old. Current wells are those that hold a current consent in 2014 (Rotorua Geothermal Current Consents – 20141104) (shown in blue in Fig. 4) or wells for which both the maximum daily intake and the date the well stopped producing are known. Old wells (shown in grey in Fig. 4) are those for which individual production rates are not known and are currently shut.

The assignment of production in the model is hindered by the lack of good records detailing the actual production of individual wells between 1950 and 1987 as the development of the field was highly unregulated. In order to represent the production history from the RGF and actual production from the geothermal bores as realistically as possible, the field was divided into five geographical zones (Fig. 6) for which total production rates had been estimated in 1985 and 1988 by Bradford (1992) (Fig. 6). The amount of production allocated to current and old wells in each geographical zone was back-calculated from 1985 to 1950 using the proportions calculated for each geographical zone in 1985 and the annual production history from the whole of the RGF

(Fig. 7).

To back-calculate production from individual wells from 1950 to 2014, additional assumptions had to be made:

- The consented maximum daily take and net abstraction provided by EBOP (Rotorua Geothermal Current Consents – 20141104) are used in the model as the actual mass withdrawn from and injected into the geothermal aquifers,
- The production for the current wells was increased by 30% before the closure to account for the fact that some consents and big users may have reduced production after the well closure,
- The proportion of production for unconsented wells is evenly distributed amongst the old wells in the appropriate geographical zone,
- All wells start producing in 1950, and
- Old wells are all shut in 1986

This is major improvement on the production scheme implemented in earlier models as it explicitly includes big users and areas of important mass withdrawal as well as giving a more realistic representation of the well closure. In addition, to represent the highly seasonal

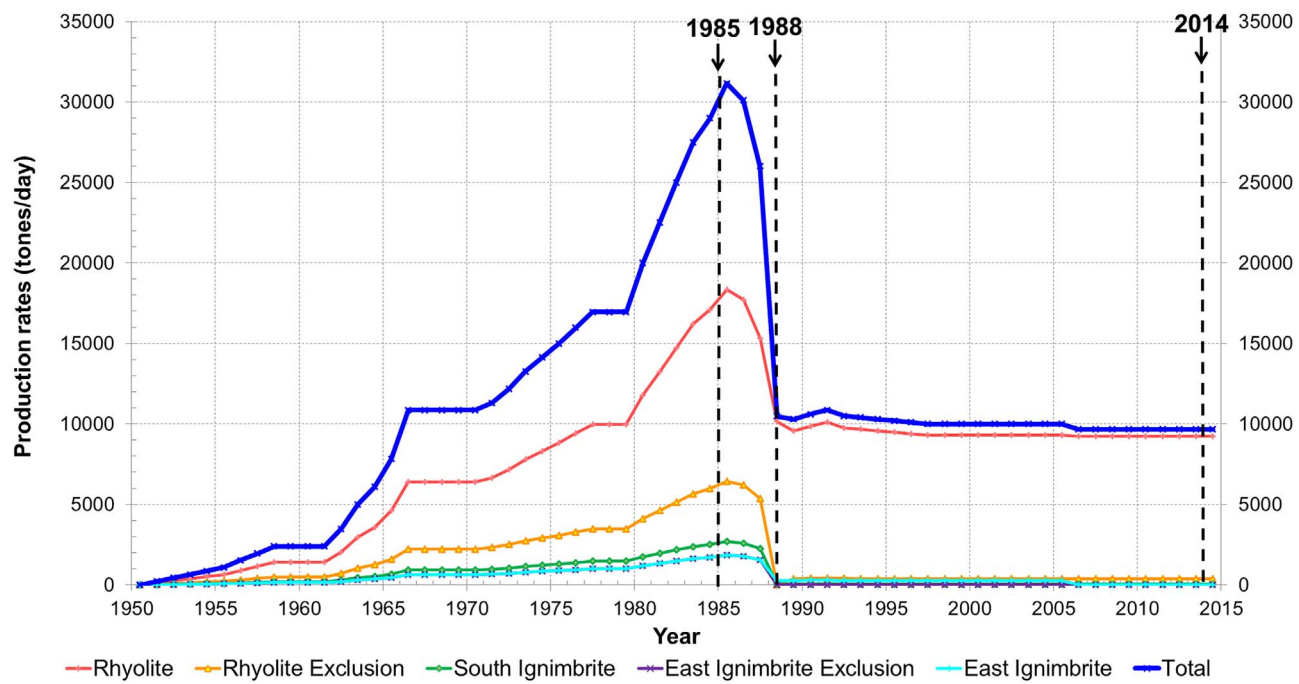


Fig. 7. Production rates allocated to each geographical zone from 1950 to 2014.

component in utility drawoff from geothermal bores in the RGF, a 20% difference between summer and winter values was used before 1991, and a 10% difference was used after 1991 to account for a change in the behaviour of well users (Fig. 5) (Bradford, 1992).

#### 4. Numerical model development

The first stage of modelling involves the creation of a conceptual model of the geothermal resource which consolidates the field data and represents our understanding of the physical processes driving the hydrothermal system. Then a three-dimensional array of blocks that covers the region of interest is generated, to which suitable numerical values are assigned to model parameters to replicate the physical processes identified in the conceptual model. Some aspects of the conceptual model, numerical model, and boundary conditions for the RGF are described in the following sections.

##### 4.1. Conceptual model of the Rotorua geothermal field

For the present study a re-evaluation of the down-hole temperature data available from bores was carried out in collaboration with GNS Science using the Leapfrog software (Milicich et al., 2005). By combining and cross referencing DSIR (Department of Scientific and Industrial Research) and EBOP databases, 191 distinct wells have been identified and referenced. Temperature profiles have been measured by DSIR and EBOP from 1953 to 2011 (80% measured in the 1980s). Along with the down-hole temperatures, surface temperature contours (where available) and surface features temperatures were included to construct three dimensional temperature contours representative of the RGF. Fig. 8.

3D temperature contours were interpolated using the Leapfrog software internal dual kriging method (Newson et al., 2012) and plan views at the surface and at 180 masl are shown in Figs. 9 and Fig. 10.

Temperature contours at 180 masl in Fig. 10 shows the main up-flow zones at Whakarewarewa, Kuirau Park, and Ngapuna indicated by temperature maxima of between 180 and 200 °C. Geothermal fluid rises from fault structures inferred by Wood (1992): N-S faults (T & S – unnamed fault postulated by Taylor and Stewart, 1987; Ngapuna and Roto-a-Tamaheke), ring faults, and SW-NE faults (Horororo) within the

Mamaku ignimbrite in the east and extreme south sections of the field (Whakarewarewa and Ngapuna) and from the Kuirau Fault underneath Kuirau Park (Figs. 10 and 11). Lower temperatures and temperature inversions in geothermal bores across the Buried Domes highlight a lateral out-flow zone leading from the up-flow zones across the rhyolite domes towards the Lake and Government Gardens. The contours at 180 masl also show colder water around the Saddle between the Buried Domes to the west of the RGF and between the Whakarewarewa region and Ngapuna area to the East of the field (Fig. 10).

The rhyolite and ignimbrite geothermal aquifers are overlaid by generally low permeability sediments of lacustrine origin (Fig. 11). This cap is breached where temperature anomalies and geothermal surface features are evident (Whakarewarewa, along the Puarenga Stream, Government Garden, Ohinemutu, and Kuirau Park) as shown by the surface temperature contours in Fig. 9.

The overall temperature contours are consistent with the conceptual model previously developed in Ratouis et al. (2016a,b), but minor changes were made to the permeability structures (fault location and sedimentary cover) to better match the high temperatures at 180 masl, particularly along the Kuirau and Ngapuna faults.

Fig. 11 shows a cross section of the updated conceptual model of the Rotorua Geothermal Field which includes the main features of the geothermal resource (the trace of the vertical section is shown in Fig. 12).

Additional information on the geological structure, geochemistry, well stratigraphy, and downhole well temperatures used to build the conceptual model is available in Ratouis et al. (2016a,b).

##### 4.2. Numerical model setup

The objective of this numerical modelling study is to provide a detailed representation of the geothermal aquifers and the near surface behaviour of discharging features at Rotorua. For these reasons, the EWASG (WAter-Salt-Gas) equation of state (EOS) developed by Battistelli et al. (1997) was used and AUTOUGH2 (Yeh et al., 2012), the University of Auckland's version of TOUGH2 (Pruess et al., 1999) was utilised as the numerical simulator. This EOS enables the representation of the shallow unsaturated zone as a mixture of water vapour and CO<sub>2</sub>. The thermophysical property correlations used in EWASG are accurate

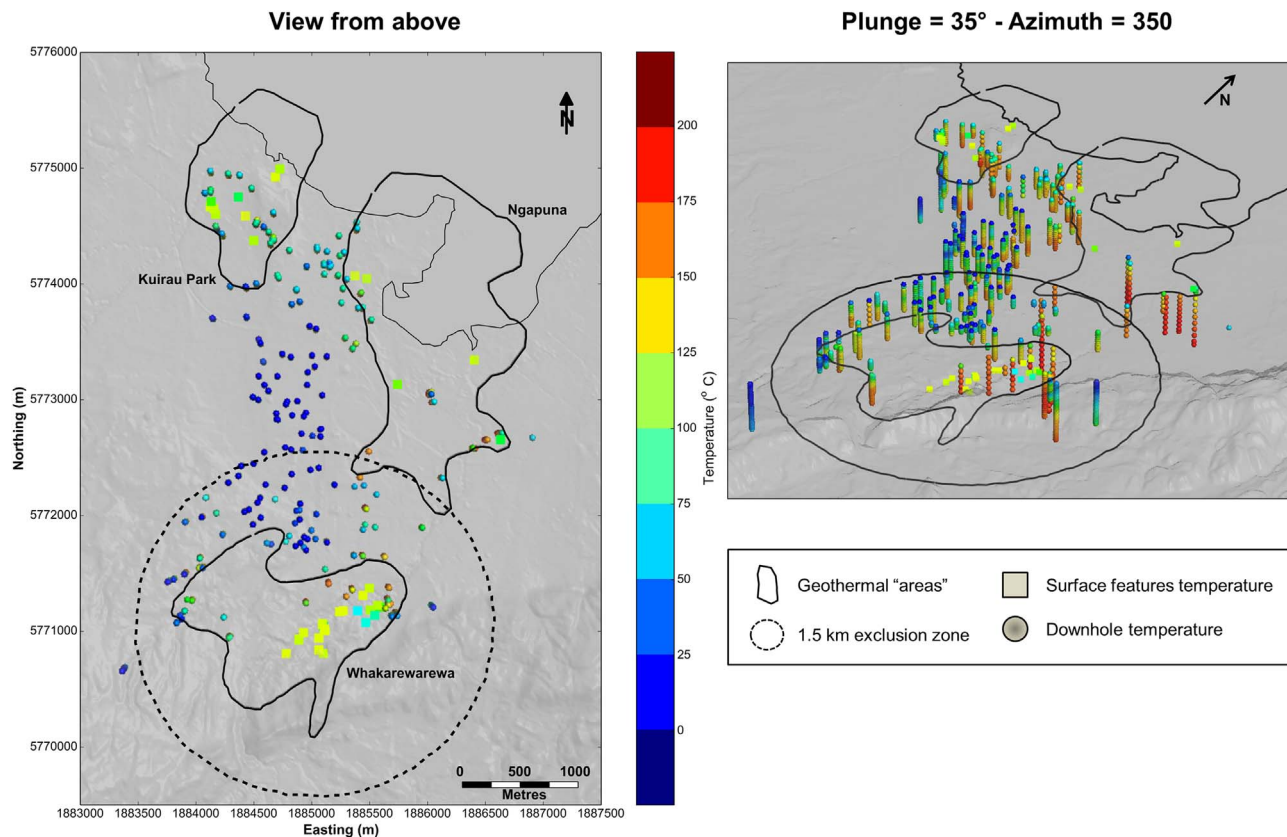


Fig. 8. Downhole temperature data and surface temperatures of the monitored geothermal features at Rotorua.

for temperatures up to 350 °C and fluid pressures up to 80 MPa. A full discussion of the thermophysical property correlations used is given in the original paper (Battistelli et al., 1997).

#### 4.2.1. Model specifications

The grid structure for the numerical model of the RGF consists of 48,034 blocks in total and is shown in Fig. 12. It is the same grid as used in UOA Model 4a (Ratouis et al., 2016a). It covers an area of 12.4 km x 18.3 km centred on the Rotorua Township with a block size ranging from 125 m × 125 m to 1000 m × 1000 m. There are 30 layers (thickness varying from 5 m to 200 m) extending to a depth of 2000 m below sea level. The geological structure of the geothermal system is defined by the numerical values of various rock-type parameters that are assigned in the model. A total of 120 rock-types were used to account for the detailed geology of the RGF. Permeability, porosity and density values assigned to the rock formations within the resistivity boundary of the geothermal system are presented in Table 1. Some formations were allocated more than one rock-type to allow for different levels of fracturing, (e.g. Utuhina rhyolite).

A thermal conductivity of  $2.5 \text{ W m}^{-1} \text{ K}^{-1}$  and specific heat of  $1000 \text{ J kg}^{-1} \text{ K}^{-1}$  were applied uniformly to all rock-types.

#### 4.2.2. Boundary conditions

**4.2.2.1. Top surface.** The top layers of the model follow the surface topography and Lake Rotorua bathymetry and an “atmosphere” block of a very large volume has been applied over each column. This approach allows differentiating between columns which are located at the surface and columns which underly Lake Rotorua. “Dry” atmosphere blocks containing CO<sub>2</sub> gas and water vapour at normal atmospheric pressure and temperature are applied over column at the surface. This allows air, CO<sub>2</sub>, and water vapour to flow freely from the “dry atmosphere blocks” into the model, and air, CO<sub>2</sub>, water vapour and/or water to flow freely out of the model into the dry atmosphere.

Whereas column located underneath Lake Rotorua have cold water at constant pressure and temperature as a top boundary condition. The values for pressure are defined by hydrostatic pressure corresponding to the depth of the lake, assuming a water temperature of 10 °C. Water can flow freely between the model and these “wet atmosphere blocks”. The very large volume used allows the conditions in these blocks (“dry atmosphere” or “wet atmosphere”) to remain constant throughout the simulation.

Annually or monthly-averaged rainfall (Fig. 3) with an infiltration rate of 10% is represented by cold water injected into the top surface blocks of the UOA Model 5. Over the urbanized zone the infiltration rate was reduced to 8% to account for paved areas and the existing drainage system.

**4.2.2.2. Lateral boundaries.** The boundaries on all four vertical sides of the model are closed – they do not allow flow into or out of the model. This is based on the assumption that the model grid area is large enough to contain the whole of the pre-production undisturbed hydrothermal system, and hence mass or heat flows at the sides of the model will be negligible.

**4.2.2.3. Base boundary.** Inflow of high enthalpy water, chloride and CO<sub>2</sub> is applied at the base of the inferred faults (Table 2) and a conductive heat flow of 80 mW/m<sup>2</sup> is applied elsewhere. These boundary conditions are the same as were used in UOA Model 4a except for the seasonal variation in rainfall.

**4.2.2.4. Production and reinjection of geothermal fluid.** Time-dependent generation rates are defined bi-annually for the geothermal bores in the RGF from 1950 to 2014 and are included in the history-matching simulations as sink and source generators. A specific enthalpy for mass injection is specified for reinjection wells for each consent (EBOP – Rotorua Geothermal Current Consents – 20141104).

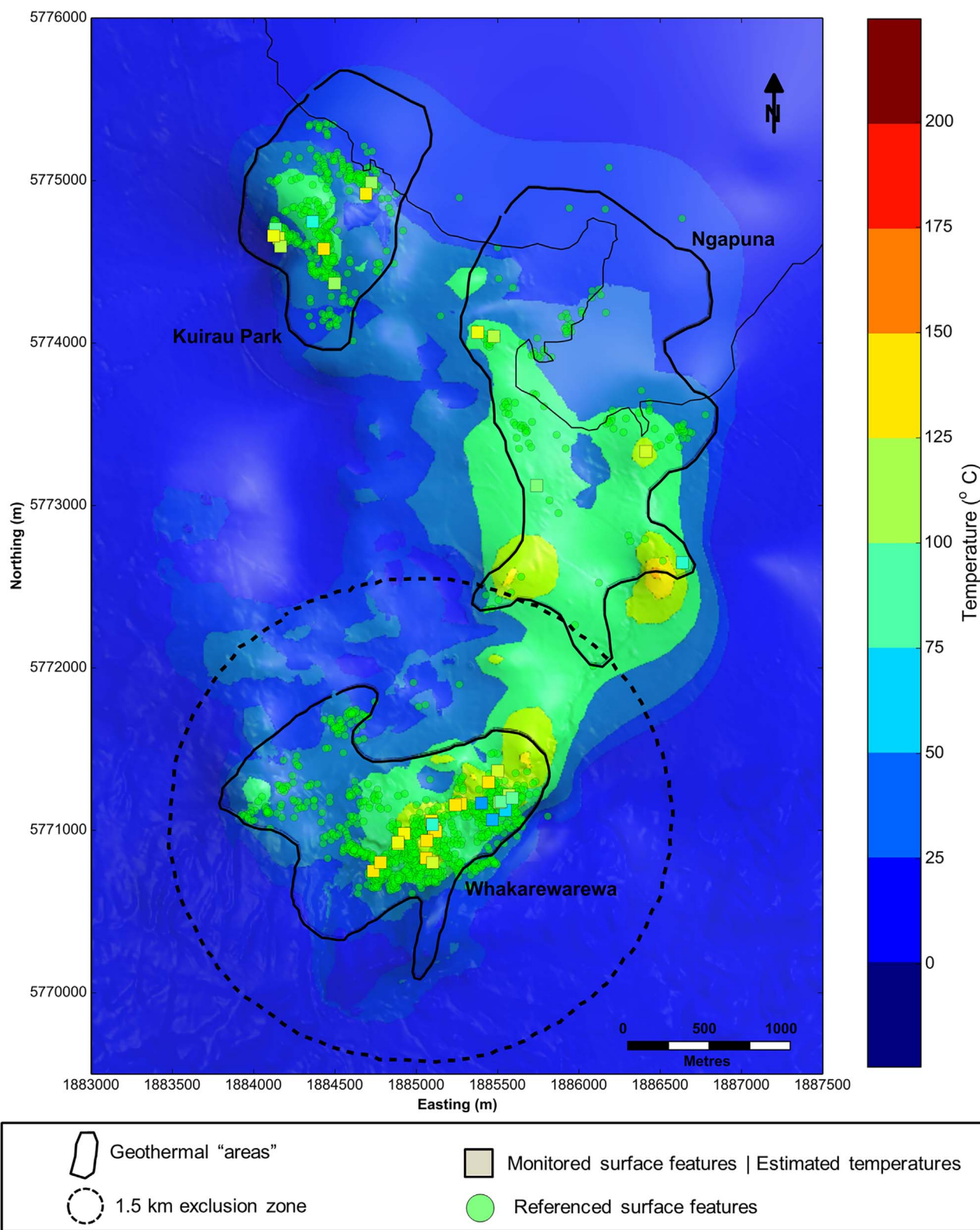


**Fig. 9.** Temperature contour map of the RGF at ground level (surface features are indicated by the colored dots).

#### 4.2.3. Other model parameter

See [Table 3](#).

#### 5. UOA model 5 simulation results

The simulations for UOA Model 5 were carried out in three distinct

stages. A first stage reproduces the “steady state” of the system (prior to 1900) to provide a set of initial conditions for the transient simulations. This is followed by a natural state model which represents the period from 1900 to 1950 for which rainfall data is available and is included as input for the history matching simulations. From 1950 to 2014, two production models, Annual Model and Seasonal Model, are run which

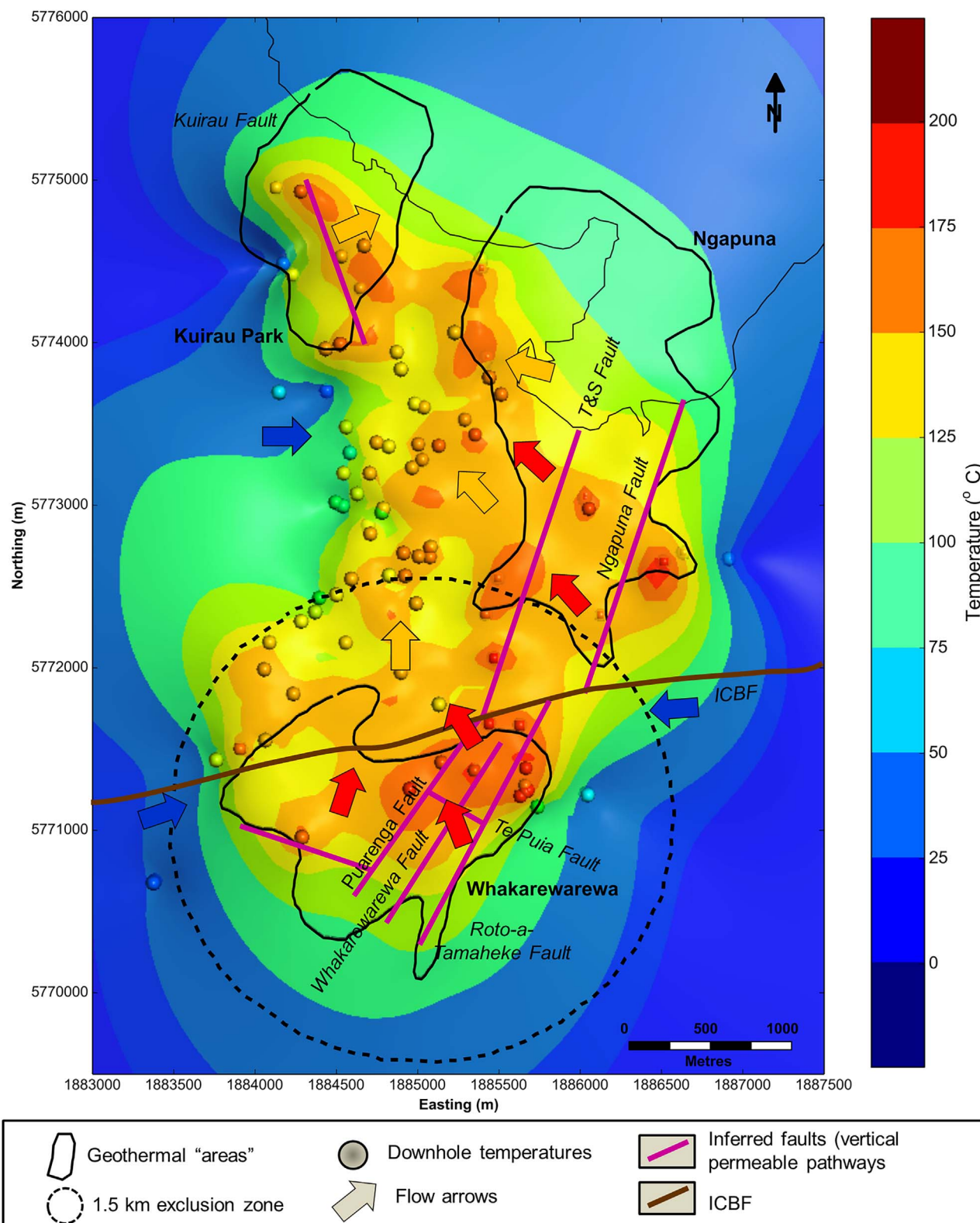


Fig. 10. Temperature contour map of the RGF at 180 masl (wells are indicated by the colored dots), including a simplified fault structure and mass flow.

include annual and monthly average of rainfall and production and reinjection from the geothermal bores, respectively to ass. The objectives of these simulations are twofold:

- To build a model which can represent flow mechanisms identified in the conceptual model of the geothermal field and to reproduce the past behaviour of the RGF (activity and spring decline, the wellbore

closure, and the more recent behaviour recorded in the monitoring wells) to constraint boundary conditions and permeability structures in the Rotorua geothermal field.

- To match the current behaviour of the surface features monitored by EBOP from 2008 and to identify potential factors impacting the activity of the geothermal features.

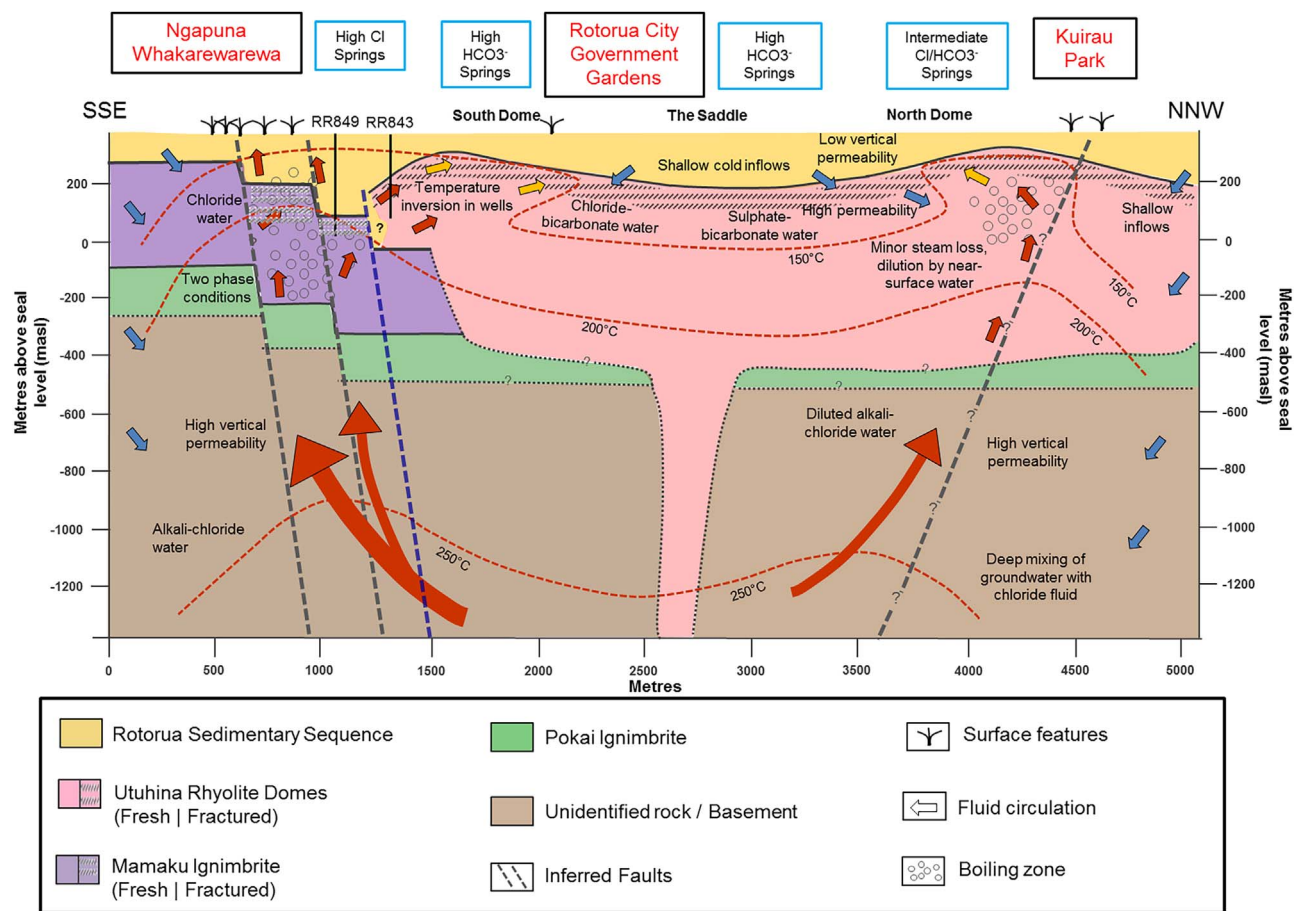


Fig. 11. NNW – SSE Cross section of the conceptual model of the RGF (color code for the arrows: red = hot geothermal fluid, yellow = warm geothermal fluid mixed with groundwater, blue = cold recharge). (For interpretation of the references to colour in this figure legend, the reader is referred to the web version of this article.)

The calibration process for UOA Model 5 (Annual and Seasonal models) is manual and includes the assignment of the sub-categories of rock-types (different set of properties) during calibration of both the steady state and the production history models. In general the steady state calibration process determines the large-scale permeability structure and the production history calibration depends more on local, near-well, structures. Most of the matches of model results with the field data (location and magnitude of surface heat and mass flow, pre-exploitation pressures, downhole temperature profiles, chloride concentration, surface CO<sub>2</sub> fluxes, and pressure transients) have not changed significantly from those presented by Ratouis et al. (2016a,b), and are not repeated here.

### 5.1. Steady state model match

Areas of surface activity in the steady state model, as shown by surface mass flows, are located within the model blocks that correspond with the known locations of features that discharge to the surface. The

most important areas of surface activity: Kuirau Park, Ohinemutu, Government Gardens, Ngapuna/Puarenga stream sector, Arikikapakapa and Whakarewarewa, are all well represented in the model (Fig. 13).

The match between the isotherms of the field data and the modelled temperatures is presented in Figs. 14 and 15.

Surface temperatures range from 17 °C to 120 °C in the field and from 15 °C to 123 °C in the model (Fig. 14). At 180 masl the field data temperatures range between 20 °C and 200 °C and modelled temperatures between 12 °C and 204 °C (Fig. 15). Mass flux arrows are plotted in Fig. 15 and show the predominant Southeast-Northwest outflow of the geothermal fluid along the Rotorua rhyolite, consistent with the conceptual model of the RGF.

The overall match is satisfactory and all areas of surface activity are represented in the model (Kuirau Park, Ohinemutu, Sulphur Bay, Whakarewarewa, and Arikikapakapa). Modelled temperatures at 180 masl south of Whakarewarewa are still too high and the model could be improved by additional calibration.

Table 1

Range of permeability values and rock density assigned to the major rock formations in UOA Model 5. (a) Hunt (1992); (b) Robert et al. (2010).

Rock-type	(x,y) Permeability [10 <sup>-15</sup> m <sup>2</sup> ]	(z) Permeability [10 <sup>-15</sup> m <sup>2</sup> ]	Porosity	Rock grain density [kg/m <sup>3</sup> ]
Sediment Sequence	8–1500	4–180	0.1	2600 <sup>(a)</sup>
Rhyolite dome (“Fresh”)	10–40	2–6	0.1	2150 <sup>(a)</sup>
Rhyolite dome “Fractured”	4500	650	0.2	2150 <sup>(a)</sup>
Ignimbrite sheet (“Fresh”)	15–150	5–13	0.1	2300 <sup>(a)</sup>
Ignimbrite sheet (“Fractured”)	200	13	0.3	2300 <sup>(a)</sup>
Greywacke basement	1	1	0.1	2600 <sup>(b)</sup>
Fault	5–100	15–160	0.1–0.2	2300–2600 <sup>(a,b)</sup>

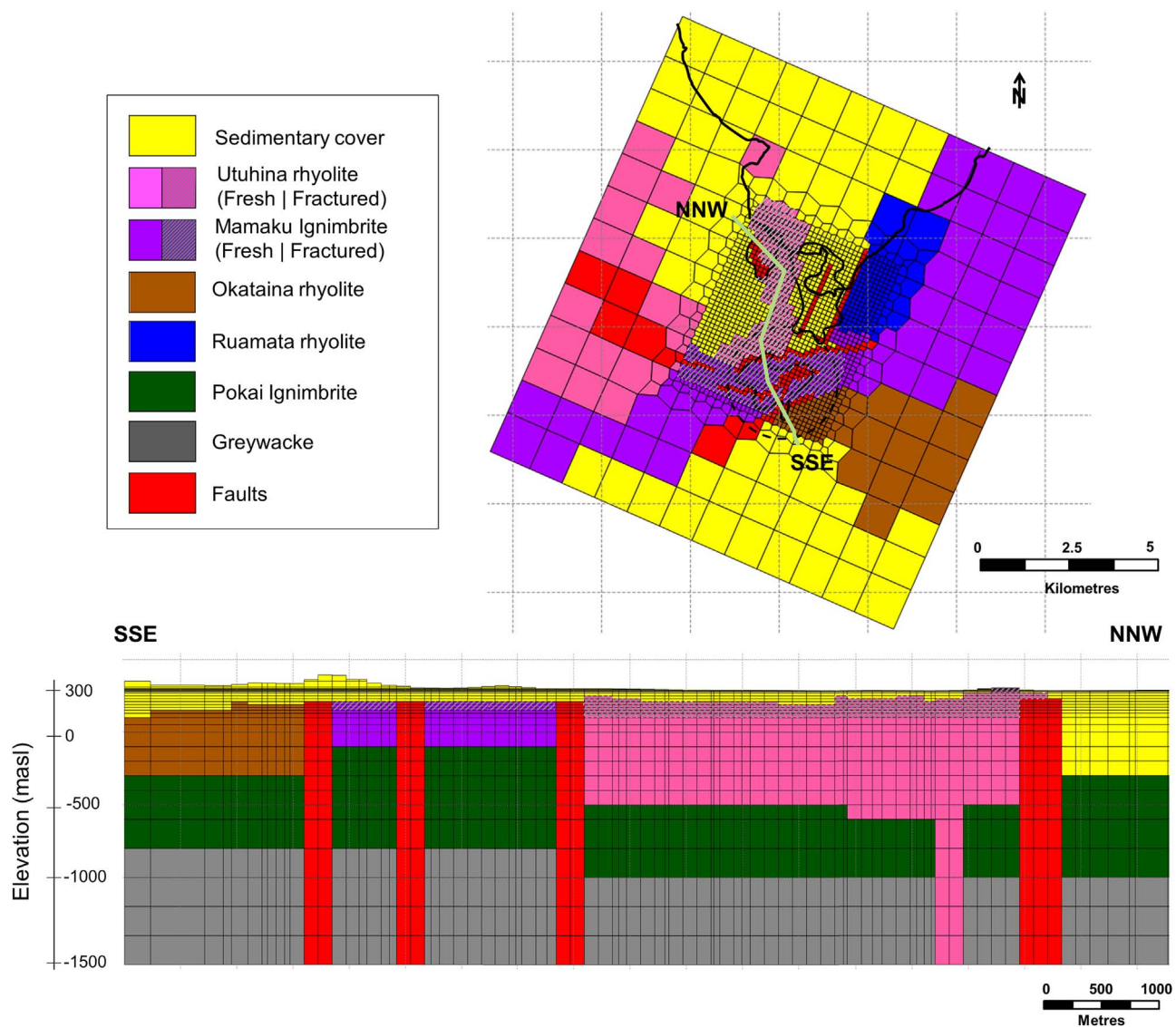


Fig. 12. UOA Model 5 plan view at 115 masl and vertical cross-section (SSE-NNW) of the model, including geology.

**Table 2**  
Deep inflows at the bottom layer of the model.

Area	Mass [t/day]	Temp [°C]
Kuirau Park	8300	255
Ngapuna Stream	23,100	270
Whakarewarewa	42,900	245
Total	74,300	

## 5.2. History matching: overall impact of the wellbore closure

### 5.2.1. Pressure response in monitoring wells

Monitoring well M12 penetrates the rhyolite aquifer and M16 the ignimbrite sheet. The historical water levels are given in Fig. 16, respectively. They are representative of the monitoring wells across the RGF which show similar behaviour:

- Decreasing water levels prior to the 1986 Bore Closure Programme,
- Fast and significant water level increases from 1986 to 1988–89, and
- Further overall increases from 1990.

Modelled and measured water levels for monitor wells M12 and

**Table 3**  
Parameters used for the UOA Model 5 simulations.

Linear equation solver
BiCGSTAB conjugate gradient solver
convergence criterion
maximum number of iterations
level of fill-in for the incomplete LU pre-conditioning
number of orthogonalizations
Other model parameters
Gravity vector
Relative permeability functions
Capillary pressure function

M16 from 1950 to 2014 are shown in Fig. 16. Results for the model with annually averaged production and rainfall (called here the Annual Model) are compared to those for the model with monthly averaged production and rainfall (called here the Seasonal Model).

Simulation results for M12 show a faster recovery than shown in field measurements and the simulated pressure drop for M16 exceeds the recorded pressure drop. However the pressure transients for both

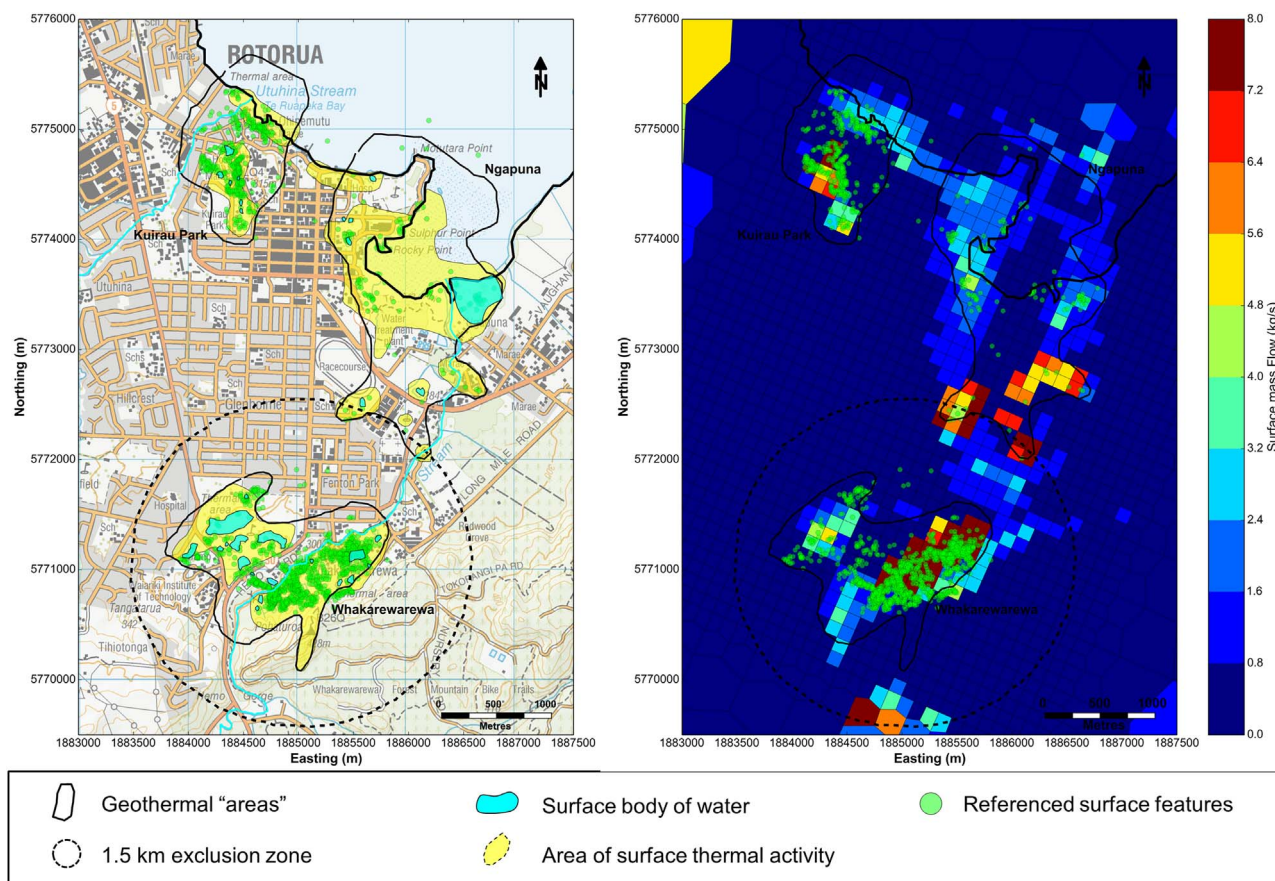


Fig. 13. Comparison between areas of geothermal surface activity and location of surface features (left) with the modelled steady state surface mass flow ( $\text{kg/s}$ ) for UOA Model 5 (right).

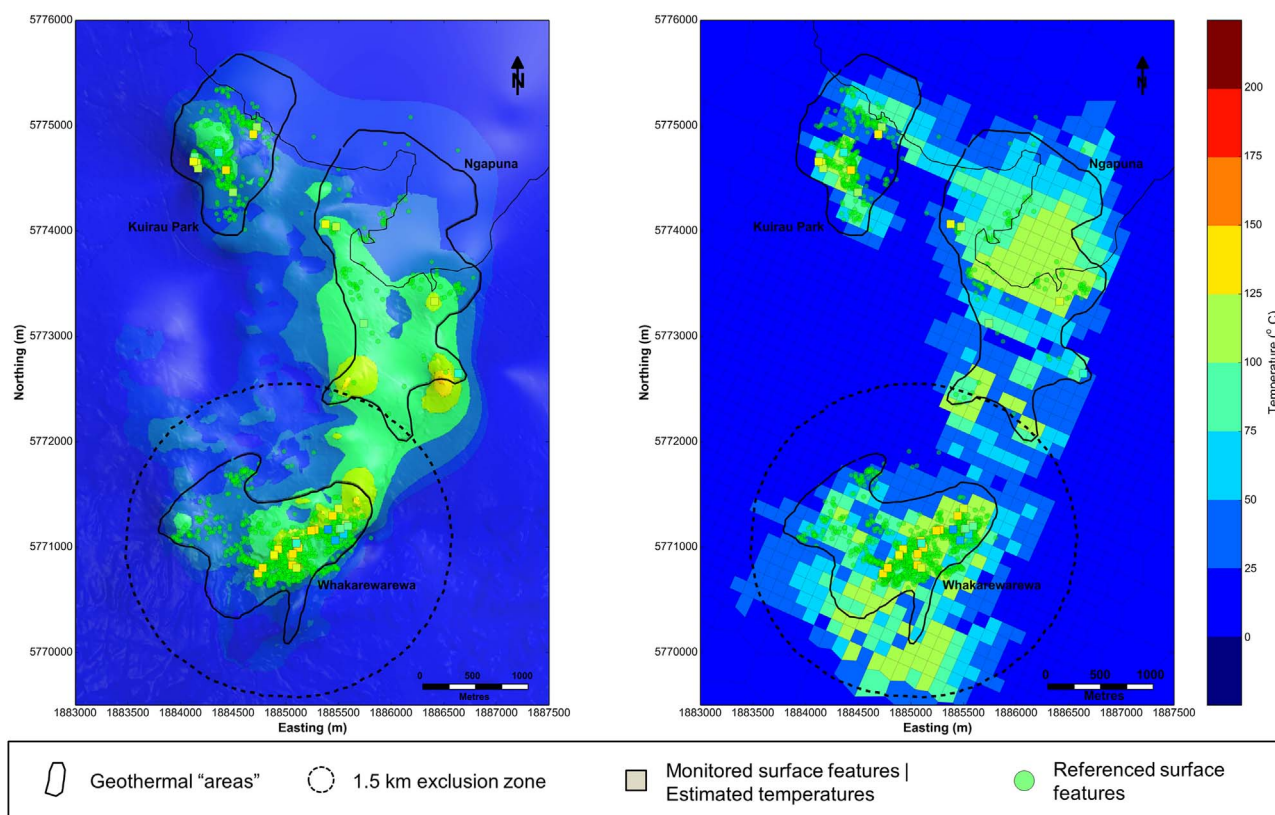
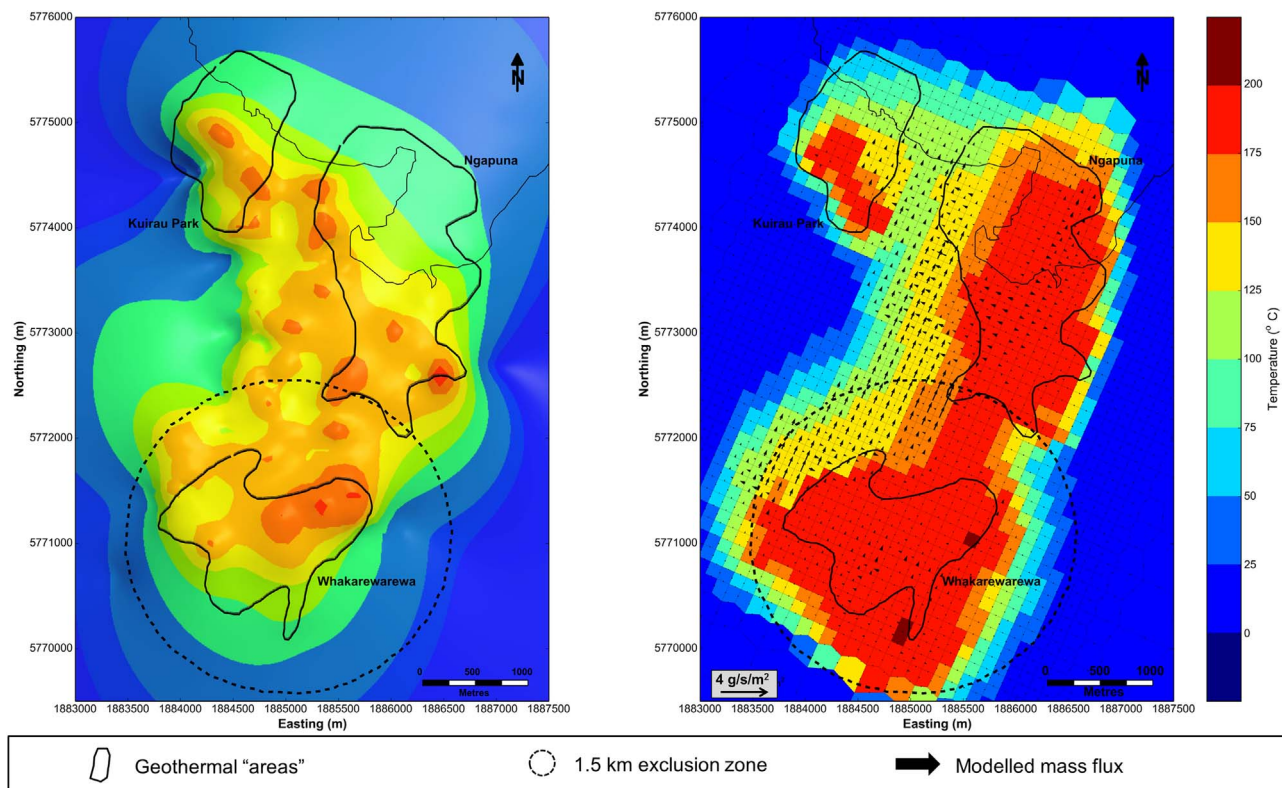


Fig. 14. Comparison between the 3D temperature contours (left) and the UOA Model 5 temperature distribution (right) at the surface.



**Fig. 15.** Comparison between the 3D temperature contours (left) and the UOA Model 5 temperature distribution (right) at 180 masl.

models quite well follow the water level trends recorded in M12 and M16.

The Seasonal Model matches pre-closure seasonal variations in both Monitor wells M12 and M16 (Fig. 17). The timing and magnitude of these variations follow the data, with pressure lows in winter. Moreover there is a strong inverse correlation between total production from the field and water levels in M12 and M16. This suggests that pressure

decreases within the geothermal aquifers and the seasonal fluctuations in pressure both have an anthropogenic origin caused by changes in utility drawoff of geothermal fluid. Following the closure, such a correlation is not clearly visible (Fig. 17). This suggests a shift in the dynamics of the geothermal system from an anthropogenic controlled system to a system less impacted by utility drawoff.

Daily-averaged pressure transients for the other M-wells can be

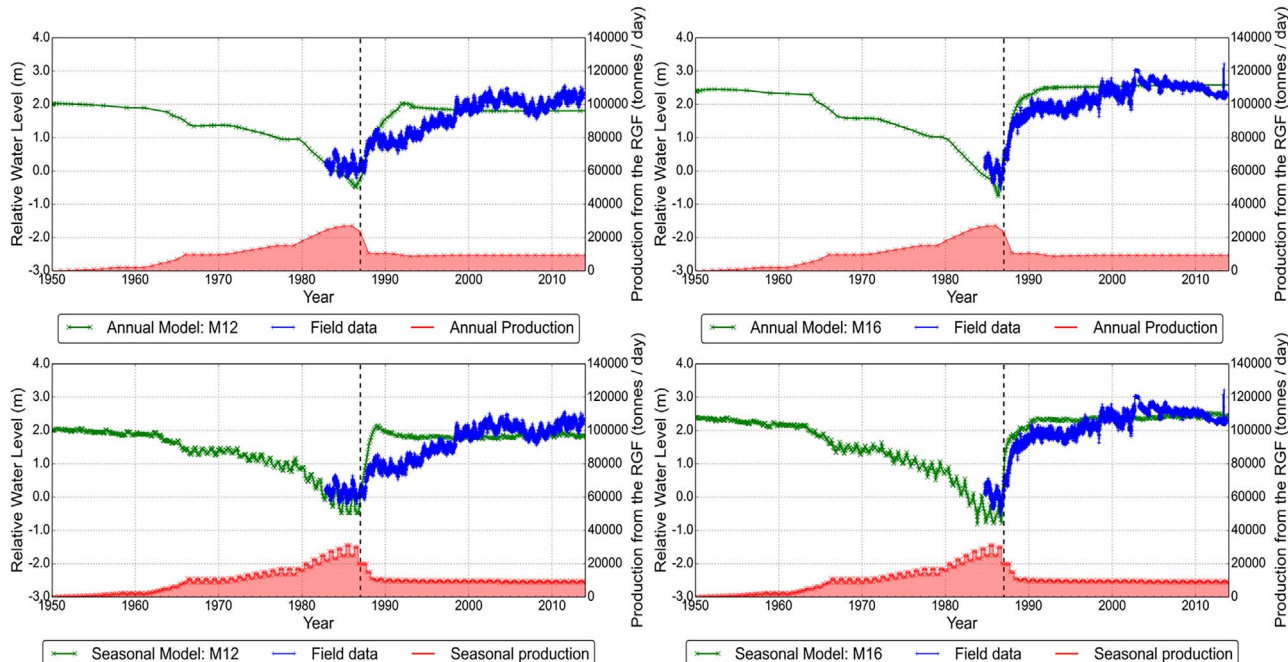


**Fig. 16.** Simulation results for Annual Model (top) and Seasonal Model (bottom) versus measured water levels from 1950 to 2015 in monitor wells M12 (left) and M16 (right). The production rates are shown in red and the Bore Closure is indicated by a black dotted line. (For interpretation of the references to colour in this figure legend, the reader is referred to the web version of this article.)

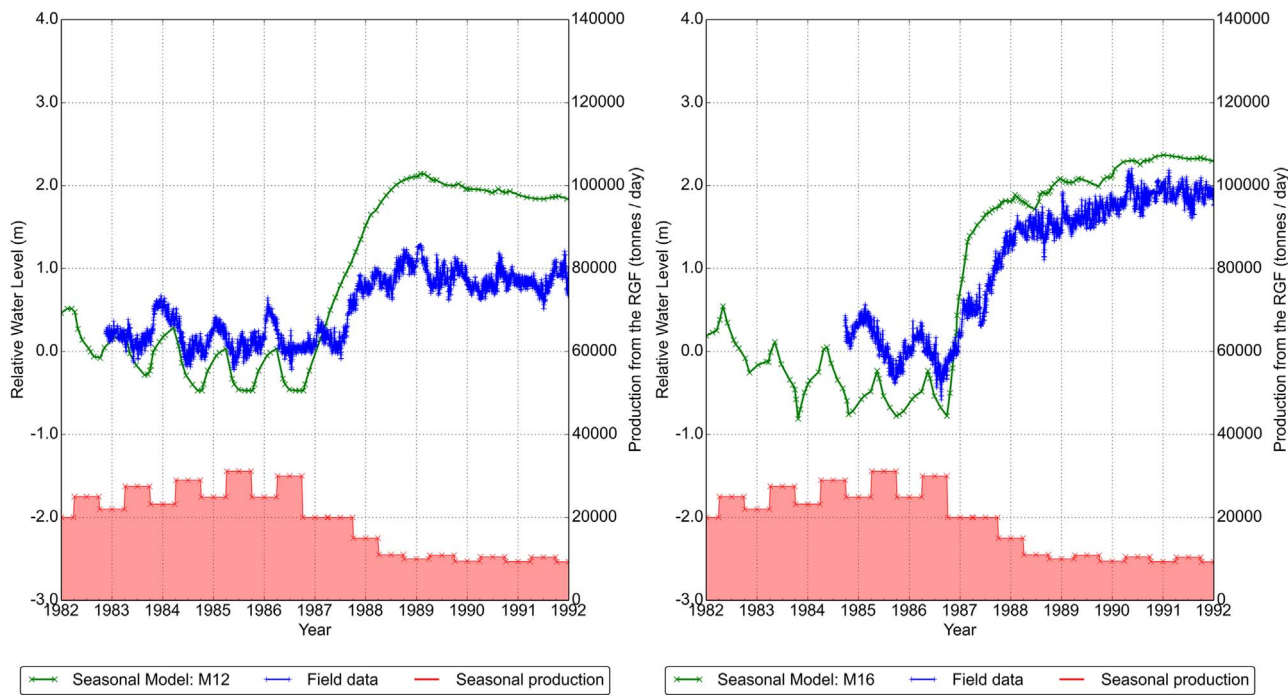


**Fig. 17.** Simulation results for the Seasonal Model versus measured water levels from 1982 to 2000 in monitor wells M12 (left) and M16 (right) (production rates are shown in red). (For interpretation of the references to colour in this figure legend, the reader is referred to the web version of this article.)

found in Gordon et al. (2005) and in GNS Science Consultancy Report (Kissling, 2014).

### 5.2.2. Changes in surface heat flow

The areas that experienced surface heat flow decline from 1950 to 1986 and recovery from 1986 to 2005 are located within Kuirau Park, Whakarewarewa and Fenton Park (Fig. 18). The model captures these general trends in surface activity and the areas affected reasonably well (Fig. 18).

### 5.2.3. Changes in modelled temperature, pressure and mass flow responses in surface features

Fig. 19 shows the modelled temperatures, surface mass flows and pressures plotted against time for the blocks corresponding to the locations of Kuirau Lake and Soda Spring within the geothermal areas of Kuirau Park and Korotiotio and FRI path within the geothermal areas of Whakarewarewa (Fig. 2). The production rates from the RGF showed in red is also included. Although limited field data are currently available for comparison, the model results are consistent with observations that

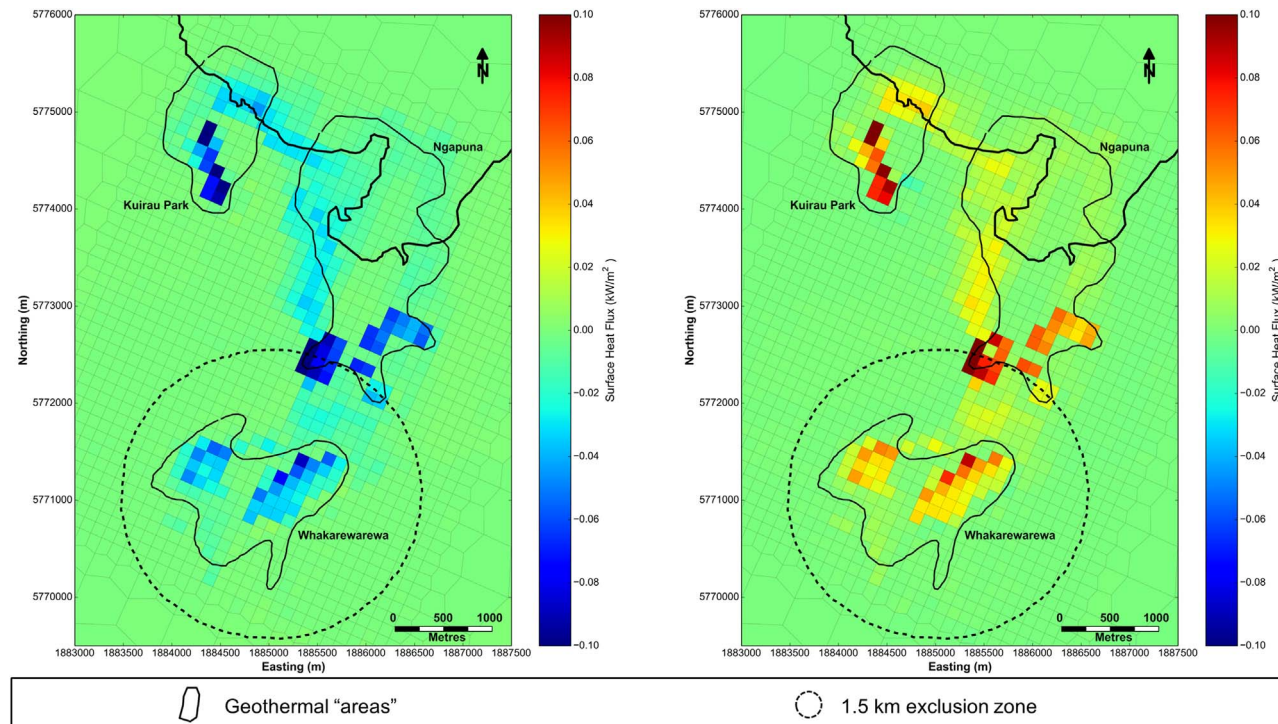


**Fig. 18.** Simulation results for heat flux decline 1950–1986 (left) and heat flux recovery 1986–2014 (right).

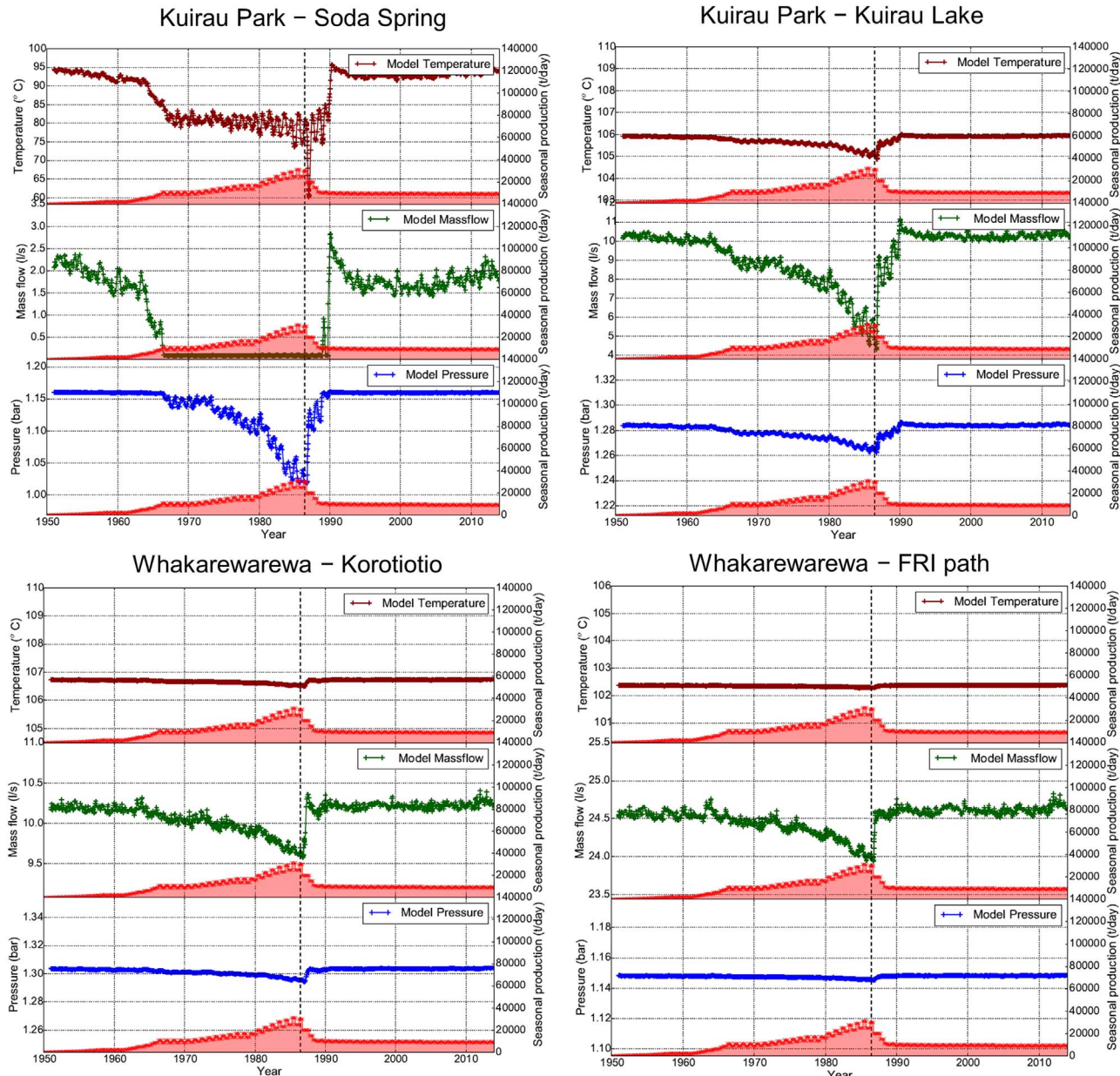


Fig. 19. Modelled temperature, mass flow and pressure for surface blocks at Kuirau Park – Soda Spring (top left), Kuirau Park – Kuirau Lake (top right), Whakarewarewa – Korotiotio (bottom left), and Whakarewarewa – FRI path (bottom right).

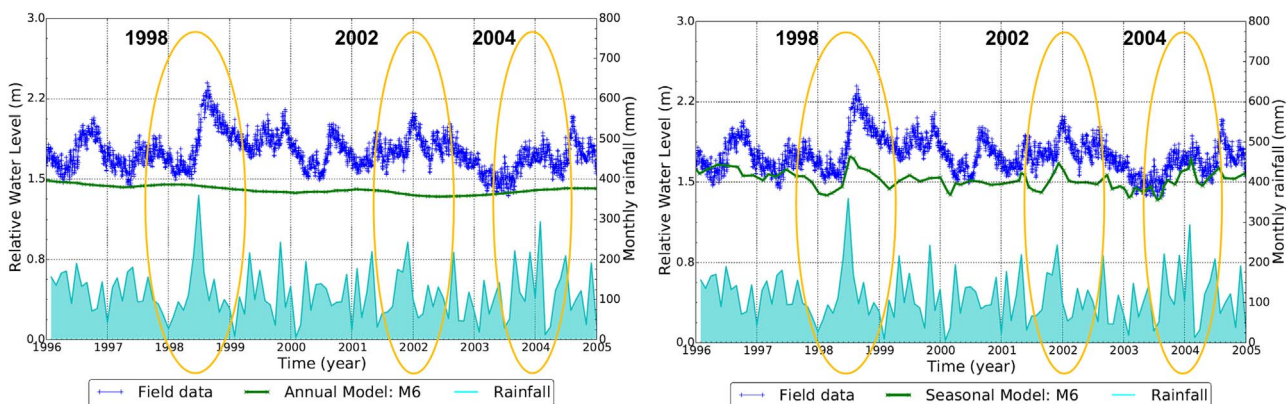
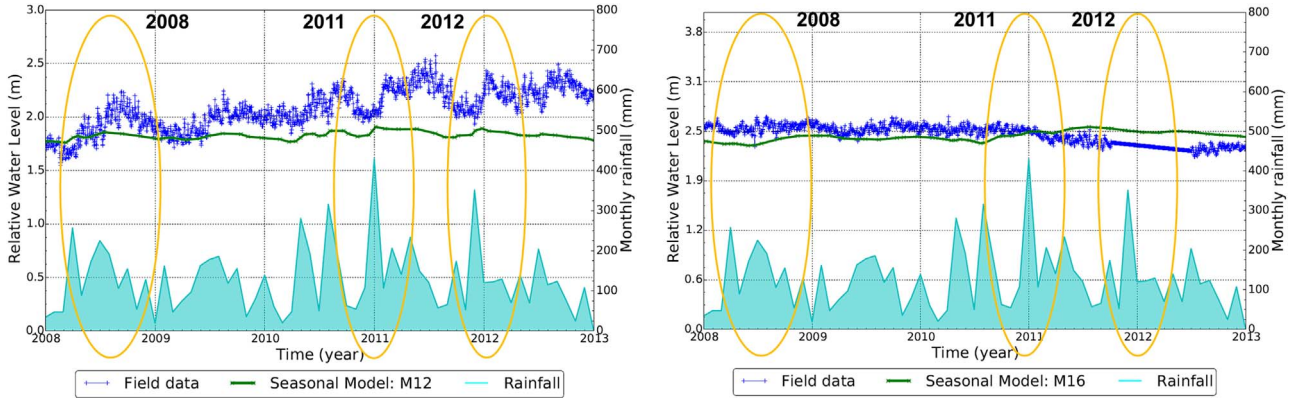


Fig. 20. Simulation results showing pressure changes and rainfall from 1996 to 2005 for monitoring well M6 for the Annual Model (left) and the Seasonal Model (right).



**Fig. 21.** Simulation results for the Seasonal Model showing the pressure changes and rainfall from 2008 to 2013 for monitoring wells M12 (left) and M16 (right).

Kuirau Park Lake essentially ceased overflowing and sinter-lined basins went dry in the early 1980s. The model shows a full recovery of surface features at Kuirau Park from 1990. This is also consistent with the field observation that these features started discharging in the 1990s with fluids which were chemically similar to those sampled in the 1960s (Mroczek et al., 2004), indicating a recovery to near pre-closure status. For surface features at Whakarewarewa simulation results shows a small decline in both fluid temperature and surface mass flow prior to the wellbore closure and fast recovery after the closure. Observations at Rotorua suggest the model underestimate the decline and overestimate the recovery of the surface features at Whakarewarewa. However there are currently no continuous records of surface features from the RGF available for comparison.

### 5.3. History matching: recent pressure transients and impact of shallow rainwater infiltration

Water levels for M6 from 1995 to 2005 and M12 and M16 from 2009 to 2013 are presented in Figs. 20 and 21, showing some of the finer details of the modelled response.

The pressure trend in the Annual Model for M6 is mostly flat and does not account for the fine details of the response of the water level to peaks in rainfall (Fig. 20, left). The Seasonal Model however matches the water level variations in M6 very closely (Fig. 20, right). The data also reveals a correlation between rainfall and water level within the geothermal reservoir. The link between the shallow groundwater and the deep geothermal aquifer has previously been mentioned in the Rotorua geothermal bore water level assessment report prepared by GNS (Kissling, 2014). The Seasonal Model is able to reproduce this behaviour well, with a clear correlation with rainfall visible for the simulation results in Fig. 20 (left). High rainfall events at the start of 1998, 2011, and 2012 which are followed by a significant increase in water level recorded in M6 are replicated in the Seasonal Model.

A similar correlation between a high rainfall event and water level increase can be seen in well M12 (Fig. 21, left). The most evident events are in 2008, 2011 and 2012, although the magnitude of the variations is underestimated (Fig. 21, left). By contrast, monitoring well M16 does not seem to be affected by such rainfall events, a phenomenon also reproduced by the Seasonal Model (Fig. 21, right).

The different types of response to rainfall in the monitoring wells M6, M12, and M16 give information on the shallow recharge of the system. Pressures from the western side of the geothermal aquifer are more correlated with rainfall than pressures from the other monitoring wells. This indicates that more rainfall flows into the system in the vicinity of well M6 (west of Whakarewarewa). This is consistent with the conceptual model of the RGF where the area known as the Saddle is believed to allow shallow recharge of the geothermal field (Figs. 10 and 11). The nearby ICBF Fault may also provide a permeable pathway for the rainfall to flow into the field. Brine chemistry (high tritium content)

of geothermal water in the vicinity of the Saddle confirms rainwater intrusion in this area (Stewart et al., 1992; Ratouis et al., 2016a).

### 5.4. History matching: recent behaviour of individual surface features

#### 5.4.1. Challenges

Forty-one surface features have had their temperature, mass flow and water level monitored by EBOP since May 2008. In the model the surface features are represented by surface blocks measuring 125m × 125m × 5m. Because of the grid size, more than one surface feature may be located in a single block which may or may not be monitored (Fig. 22). This makes it challenging to accurately quantify and compare temperatures or total mass flows.

#### 5.4.2. Modelled versus measured temperature and mass flow of surface features

We compared the temperatures and the mass flowing into the atmosphere of the surface block from the history matching simulations to the temperatures and mass flow recorded during the monitoring programme. However these values cannot be compared immediately as the temperature of the surface block is calculated at its centre and cooling of the fluid at the surface by boiling, conduction, and radiation is not considered. Also the model only takes into account the small portion of rainfall (8–10%) that infiltrates into the subsurface and ignores the effect of rainwater runoff which is believed to impact temperature variations in geothermal surface features (Leaver, 2006). Therefore the modelled temperature of the block can be significantly higher than the temperature of the spring recorded at the surface by EBOP. In addition the temperature calculated in the model is effectively the average of the temperatures of all the surfaces features in the block and of the surrounding terrain. This averaging effect means that the magnitude of the temperature variations recorded in the surface features may be significantly larger than those predicted in the corresponding model block.

In order to include these effects a simple post processing tool was developed. The model proposed below is simple enough so that it can be applied as a post-processing tool, run after the reservoir simulation is complete. The corrected enthalpy for each surface feature can be written as a function of the enthalpy and mass flow in the corresponding surface block and of the rainfall in the following form:

$$h = \frac{\bar{m}_{model} h_{model} + x \bar{m}_{rain} h_{rain}}{\bar{m}_{model} + x \bar{m}_{rain}} - c \quad (1)$$

where  $h$  is the enthalpy of the surface feature corrected for the averaging and rainwater effects,  $h_{model}$  is the enthalpy of the surface block in our model,  $\bar{m}_{model}$  the mass flow of the hot fluid through the top boundary of the surface block calculated in the simulation,  $h_{rain}$  and  $\bar{m}_{rain}$  are the enthalpy and mass flow of the rainfall runoff,  $x$  is a calibration parameter representing the dilution due to rainfall runoff

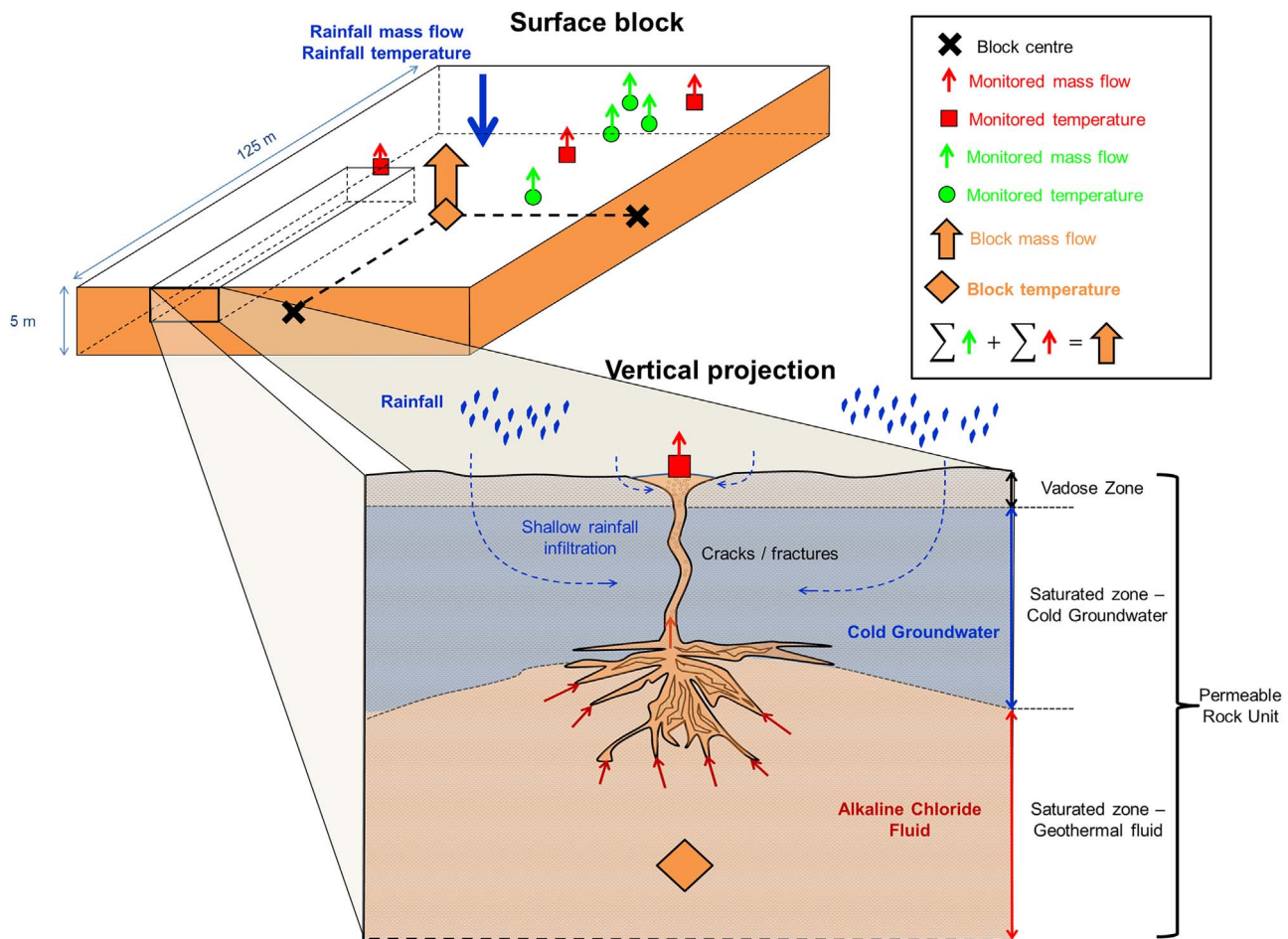


**Fig. 22.** Schematic illustration of the challenges of matching discrete surface features in a model: side view of a surface model block (top) and vertical projection of a section of the surface block (bottom). Known geothermal features are represented by green circles and monitored features by red squares. (For interpretation of the references to colour in this figure legend, the reader is referred to the web version of this article.)

entering the surface feature and  $c$  is a calibration parameter representing heat losses from boiling, conduction, and radiation.

Similarly the mass flow from the model block calculated in the simulation and can be thought of as the sum of mass flows from the surface features (monitored or not) located within the block. Therefore only a fraction  $Y$  of the total mass flow going out of the block correspond to the mass flow discharged from a particular geothermal surface feature.

$$\bar{m} = Y(\bar{m}_{\text{model}} + x\bar{m}_{\text{rain}}) \quad (2)$$

Where  $\bar{m}$  is the mass flow for the individual spring,  $\bar{m}_{\text{model}}$  is the mass flow of the hot fluid through the top boundary of the surface block calculated in the simulation,  $\bar{m}_{\text{rain}}$  is the mass flow of the rainfall runoff, and  $Y$  is the proportion of the mass flow leaving the model block that contributes to the individual surface feature.

#### 5.4.3. Enthalpy results

For all 41 thermal features a different set of parameters ( $x$ ,  $c$  and  $y$ ) were chosen to match the monitoring data as closely as possible to account for local groundwater and surface flows.

The post-processing model was applied to the model temperatures and surface mass flows for the blocks containing the surface features monitored as part of the RGMP (locations in Fig. 2). As described above, the calibration parameters ( $x$ ,  $c$ , and  $y$ ) were then determined to obtain the best match with the field data. The following figures compare the enthalpy of the numerical model block, the post-processing model and the recorded field data for selected surface features. The rainfall during the monitoring period is also included. The results are organized in four

sections depending on the quality of the match between the surface feature behaviour and the post-processing model results.

**5.4.3.1. Good matches.** For these features, the post-processing model produces a good match with enthalpy trends and amplitudes of enthalpy variations from April 2008 to January 2014 (Table 4).

Fig. 23 shows the post-processing model enthalpies and the field data curves for four surface features in Rotorua (RRF0076 – Te Horu, RRF0601 – Kuirau Lake, RRF3175 – Postmaster, RRF0283 – Korotiotio). The model results show a close agreement with measured enthalpies, with high rainfall events linked with low enthalpies. The post-processing model parameters ( $x$  and  $c$ ) are indicated in Fig. 23. For Te Horu, Kuirau Lake, Postmaster and Korotiotio the dilution factors with rainwater  $x$  are equal to 1.5, 0.8, 0.11, and 0.065 and correction factors  $c$  are equal to 110, 150, -35, and 20 kJ/kg respectively. Thus the simple post-processing model results accurately match the behaviour of these surface features.

In some instances, the parameter  $c$ , corresponding to additional cooling of the surface features outflow, is negative (Fig. 23 – Postmasters) showing that the enthalpy of the surface block is underestimated in the model. It may indicate that the model requires additional calibration (to increase the temperature of the block) or that the actual feed of the springs may be located deeper in the ground and is not estimated properly by the flow from the model surface block. This information is very useful regardless of the fact that a negative value for parameter  $c$  does not have a physical meaning in terms of the additional cooling of the surface features as described in our post-processing model.

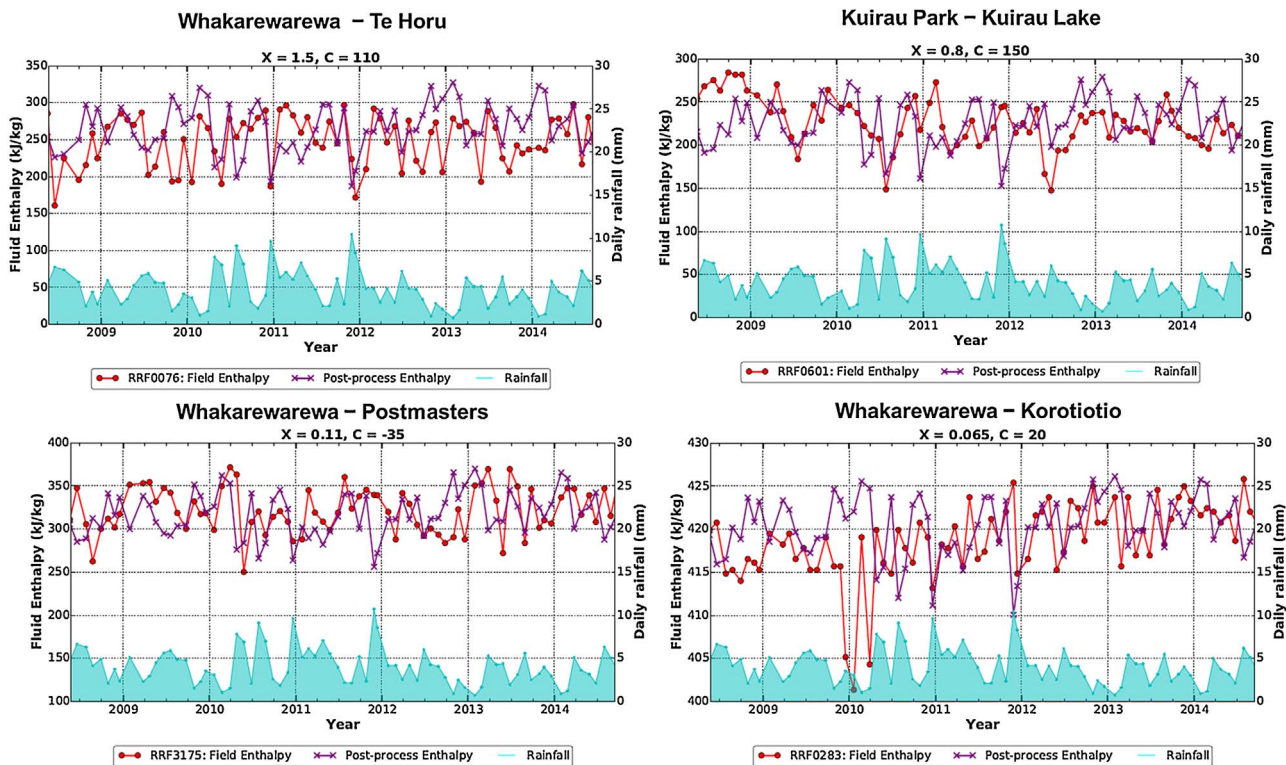


Fig. 23. Good Match – Comparison between the post-processed modelled and measured enthalpy for: Whakarewarewa – Te Horu (top left), Kuirau Park – Kuirau Lake (top right), Whakarewarewa – Postmasters (bottom left), and Whakarewarewa – Korotiotio (bottom right).

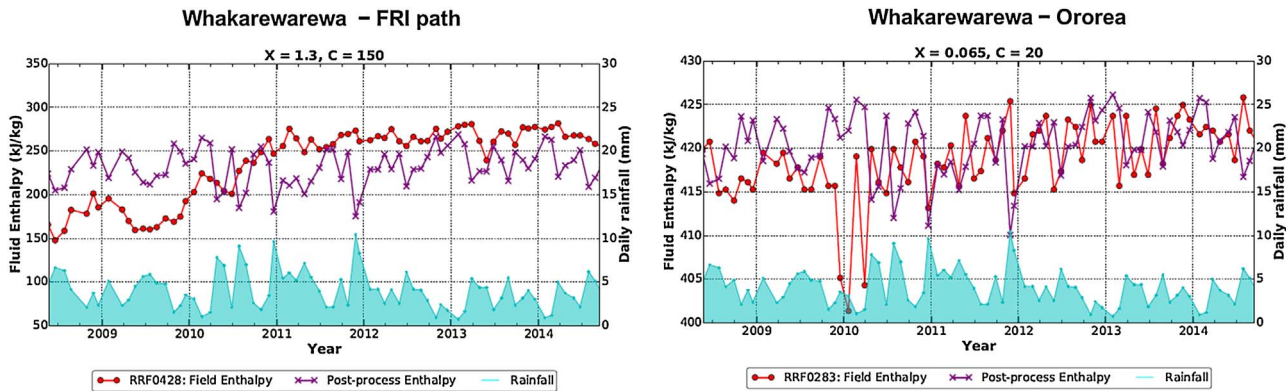
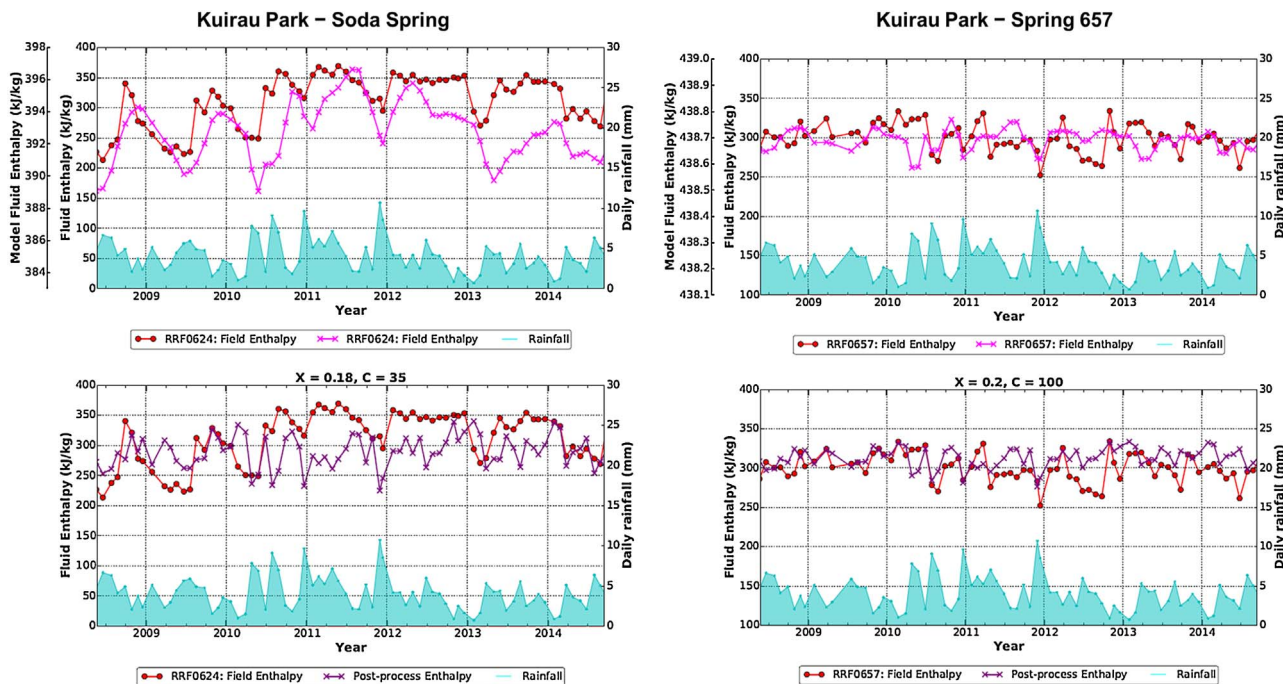


Fig. 24. Fair Match – Comparison between the post-processing model results and measured enthalpy for: Whakarewarewa – FRI path ( $x = 1.3, c = 150$ ) (left) and Whakarewarewa – Oorea ( $x = 1.0, c = 60$ ) (right). Both data sets show a change in the activity of the surface feature.

**5.4.3.2. Fair match.** For these features, the post-processing model enthalpies offer a fair match to the recorded enthalpies from April 2008 to January 2014 (Table 4). In some cases the post-processing model results produce a good match to the data for only a portion of the total measurement period. This may reflect a change in the behaviour (increasing or decreasing trends) in the surface features which is not captured in our simulations. These changes are not directly correlated with rainfall variation and instead relate to changes in the deeper feeds of the springs which potentially reflect the natural variability of geothermal surface features, changes in subsurface flow pathways, or ongoing recovery of the field. For example, the modelled enthalpies match well the enthalpy of surface feature RRF0428 – FRI path very well up to 2010 (Fig. 24). However in 2010 the surface features experienced an increase in enthalpy (90 kJ/kg) that is not represented in our model. This temperature increase is not related to the rainfall or to a change in production nearby. Similarly the enthalpy variations recorded for surface feature RRF0351 – Oorea are replicated in the post-processing model from April 2008 to approximately April 2011

(Fig. 24). From April 2011, the enthalpies drop to a lower value ( $\approx 175$  kJ/kg), an effect which is not replicated in our model.

For other surface features, the variation of enthalpy in the surface block in the original model (no mixing with rainwater,  $x = 0$ ) seem to provide a better correlation to the recorded enthalpies (this behaviour is indicated by a  $\diamond$  in Table 4). For Soda Spring located in Kuirau Park, some of the enthalpy variations in the post-processing model enthalpy have an opposite trend to the field data (indicated periods in Fig. 25, Soda Spring). The measured enthalpies for Soda Spring (RRF0624) are more correlated with changes in the original model block temperatures, though the model block is hotter and the amplitude of the variation is more than an order of magnitude smaller than the measured data (Fig. 25, Soda Spring). A similar observation applies for Spring 657 (RRF0567) also located in Kuirau Park (Fig. 25, Spring 657). These observations indicate that rainfall does not have a major impact on the behaviour of the surface feature and that it is more controlled by the deeper reservoir which is in turn affected by recharge and production from geothermal bores. A correlation between temperature variations



**Fig. 25.** Fair Match ◇. Comparison between the recorded enthalpy and the original modelled enthalpy (top) and the post-processing model results (bottom). Kuirau Park – Soda Spring ( $x = 0.18, c = 35$ ) (left) and Kuirau Park – 657 ( $x = 0.2, c = 100$ ) (right).

at Kuirau Park (including Soda Spring and Spring 657) and production from neighboring wells was proposed by Soengkono et al. (2001), which seem to be replicated in our model. To achieve a better match to the data, a deeper feed could be used in the post-processing model. A fracture flow, dual porosity, model could also be useful for investigating the potential impact of changes in production on the surface features.

**5.4.3.3. Poor match.** For these features, the post-processing model enthalpies offer a limited match to the recorded enthalpies in the surface features from April 2008 to January 2014 and their behaviour is not well represented (Table 4). This can be caused by cyclic behaviour or increasing/decreasing trends that are not shown by our post-processing model results or for recorded enthalpy variations that are not correlated to the enthalpies in our simulations (Fig. 26).

The following table summarizes the long-term behaviour trends (defined in Pearson-Grant et al., 2015) and the quality of match with

our post-processing model for forty surface features at Rotorua .

#### 5.4.4. Mass flow results

The correlation between simulation results for mass flow and recorded mass flow is not clear for most surface features (Fig. 27). There are several difficulties faced when attempting to match measurements of discharging surface features, which may explain the lack of a conclusive match between modelled mass flows and observations:

- Limited data points
- High variability
- Lack of precise measurements

Moreover field measurements of the surface feature mass flows do not include losses by vaporization and shallow seepage. For example Korotiotio (Fig. 27), Korotiotio which is a large boiling alkali spring

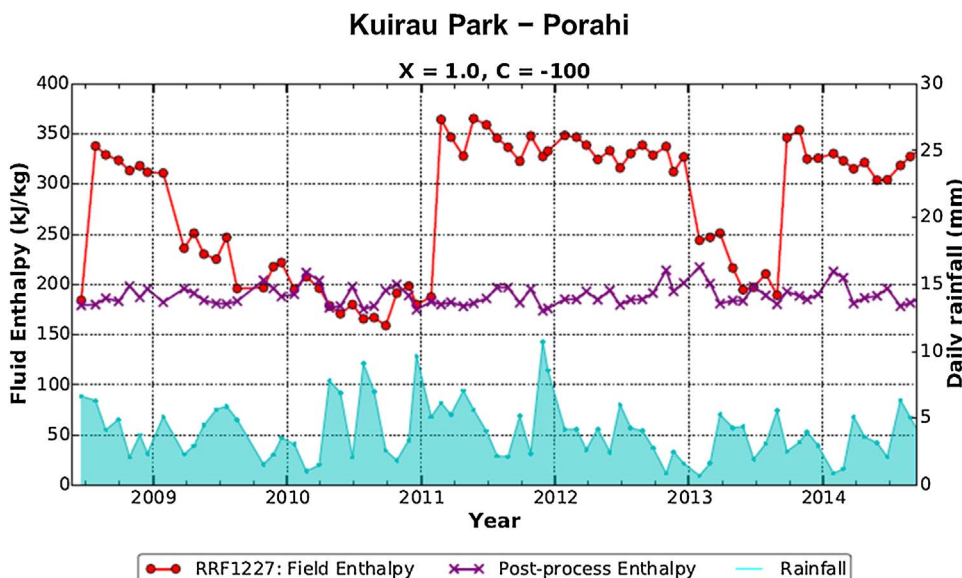


**Fig. 26.** Poor Match – Comparison between the post-processed modelled and measured enthalpy for Kuirau Park – Porahi showing cyclic behaviour not reflected by the model ( $x = 1.0, c = -100$ ).

**Table 4**

Quality of matches between the geothermal features and the post-processing model. A description of the behaviour of the selected surface features is also given (Pearson-Grant et al., 2015). Surface features with no visible trend due to lack of data are reported in the table as N/A.

Feature ID	Name	Zone	Spring/Geyser behaviour	Quality of match
RRF0529	Ngararatuatara	Whakarewarewa	Steady	Good
RRF0028	Papakura	Whakarewarewa	Increase	Poor
RRF0126	Waikite geyser	Whakarewarewa	N/A	Fair
RRF0122	Pareia	Whakarewarewa	N/A	Good
RRF0072	Prince of Wales Feathers	Whakarewarewa	N/A	Limited data
RRF0077	Waikorohihi	Whakarewarewa	N/A	Good
RRF0078	Mahanga	Whakarewarewa	N/A	Good
RRF0278	Kereru	Whakarewarewa	N/A	Limited data
RRF0079	Wairoa	Whakarewarewa	Increase	Fair ♦
RRF0081	Puapua	Whakarewarewa	Steady	Fair
RRF0076	Te Horu	Whakarewarewa	Perturbed	Good
RRF0075	Pohutu	Whakarewarewa	N/A	Limited data
RRF0055	55	Whakarewarewa	Steady	Fair
RRF0283	Korotiotio	Whakarewarewa	Steady	Good
RRF0337	Roto-a-Tamaheke	Whakarewarewa	Increase	Fair ♦
RRF0352	Waipatuhuka	Whakarewarewa	Perturbed	Fair
RRF0284	Parekohoru	Whakarewarewa	Increase	Good
RRF0952	THC blowout	Whakarewarewa	Steady	Fair
RRF0488	Okianga	Whakarewarewa	Decrease	Poor
RRF0426	426	Whakarewarewa	Increase	Fair
RRF0328	Downbath	Whakarewarewa	Perturbed	Good
RRF0624	Soda spring	Kuirau Park	Increase	Fair ♦
RRF0601	Kuirau Lake	Kuirau Park	Decrease	Good
RRF0657	657	Kuirau Park	Steady	Fair ♦
RRF3170	Hamiora	Ngapuna	Steady	Limited data
RRF3171	Stopbank	Ngapuna	Perturbed	Limited data
RRF3175	Postmasters	Ngapuna	Steady	Good
RRF3177	Malfroyo geyser	Government Gardens	Cyclic	Fair
RRF3178	Rachels	Government Gardens	Perturbed	Poor
RRF1227	Porahi	Ohinemutu	Cyclic	Poor
RRF1215	Little Waikite	Ohinemutu	Steady	Good
RRF0650	649and650	Kuirau Park	Increase	Fair
RRF0715	Mayors mouth	Kuirau Park	Perturbed	Poor
RRF3014	722-2	Kuirau Park	Steady	Fair ♦
RRF0653	Tarewa spring	Kuirau Park	Increase	Fair
RRF0053	53	Whakarewarewa	Steady	Good
RRF0351	Ororea	Whakarewarewa	Perturbed	Fair
RRF0505	505	Whakarewarewa	Steady	Fair ♦
RRF3237	Pahopeke	Whakarewarewa	Perturbed	Limited data
RRF0428	FRI path	Whakarewarewa	Perturbed	Fair

that has no measured mass flow (Pearson-Grant et al., 2015). However, while its water level is approximately 1 m below the surrounding terrain and it does not obviously overflow, recording its mass flow as zero neglects the mass flow from vaporization and possible seepage to the neighboring Puarena stream. More accurate estimates of the mass flow for the features are needed for comparison with model results and for the development of more accurate models.

## 6. Discussion

Geothermal features are sensitive to damage from external factors

such as geothermal fluid extraction from an underlying geothermal reservoir. Wells may directly compete with these natural features by extracting water from the same source that supplies them. The extraction of fluids from the reservoir also induces a drop in the water levels and reservoir pressures. This causes a reduction in the amount of hot water available to flow to the surface. Boiling alkaline-chloride water springs and geysers found at Rotorua derived directly from the reservoir fluids are especially at risk. In addition geysers typically operate at very low pressures, typically < 10 KPa (Cody, 2007). Therefore, a pressure fall of a few KPa may be sufficient to permanently stop boiling at depth and subsequently geysers from erupting (Cody, 2007; Saptadji et al.,

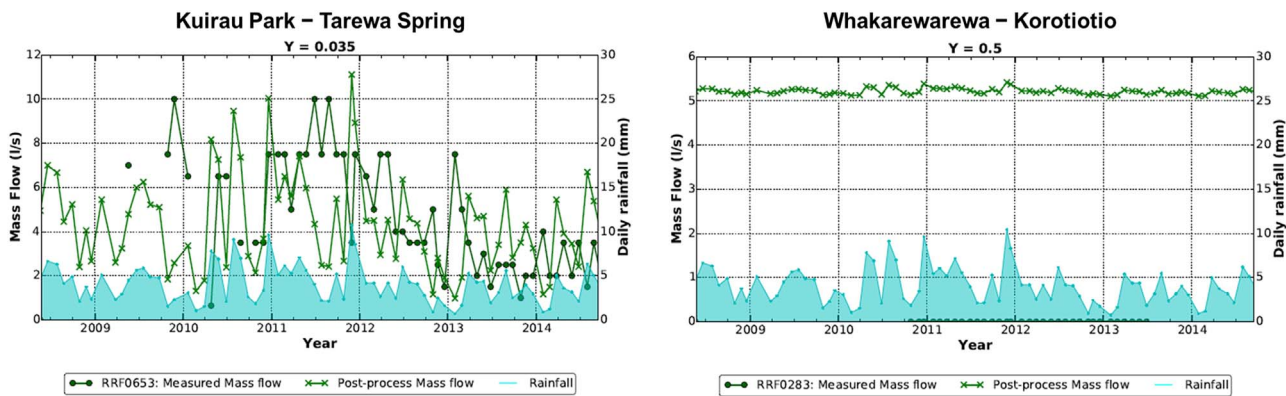


Fig. 27. Comparison between the post-processed modelled and measured mass flows for Kuirau Park – Tarewa spring ( $Y = 0.035$ ) (left) and Whakarewarewa – Korotiotio ( $Y = 0.5$ ) (right).

2016). Similarly it has been found that most hot flowing springs also operate at very low pressures, typically of only c. 3 kPa (Cody, 2007). Therefore small pressure drop as observed in Rotorua prior to the Wellbore Closure (0.1–0.2 bar) may explain the widespread decline in surface activity with many geyser ceasing to erupt and springs failing in the 1970s. Model results in Section 5.2 shows that this phenomenon is replicated (to some extent) by the model: a pressure drop in the geothermal reservoir induced by well mass extraction causes a decline in surface heat flow and surface mass discharge from most geothermal features. Currently this effect is underestimated by the model as only a few of the monitored surface features have stopped over-flowing in the model (Fig. 19). However the overall average effects of reservoir management on different reservoir areas seem to be reasonably well reproduced in the model. Additionally the results in Section 5.2 show that in order to replicate some of the pressure variations recorded in monitoring wells prior the Wellbore Closure, a seasonal component in the production is required.

Section 5.3 shows that in order to capture some of the finer scale changes in pressure variations after the Wellbore Closure, seasonal rainfall must be included.

Section 5.4 shows that by using a simple cooling post process method, the model is able to produce for 30% of the features monitored a good match, for 42.5% a fair match, for 12.5% a poor match and for 15% the limited data has hindered the modelling efforts. Therefore for some geothermal features, the model replicates current behaviour and may be able to represent realistically the response in a change of management plan. However reliable modelling of individual surface features still remains to be achieved. It is an area of current work and some progress has been made (Ratouis et al., 2016b). Assigning surface features as shallow “well on deliverability” may better represent better the structure of the surface features (feedzone plus vertical high permeability cracks to the surface) and its response to small variations in reservoir pressures.

## 7. Conclusion

A new model of the Rotorua geothermal field has been developed that better represents the shallow temperatures and includes the seasonal variations that impact the geothermal system. Results presented here confirm that seasonal variations such as the seasonal changes in production/reinjection history and rainfall must be included in the model in order to match well the behaviour of Rotorua geothermal field.

The model replicates the inverse correlation between total production from the field and water levels seen in the monitor wells before the bore closure. Following the closure such a correlation is not clear and it was found that variations in water levels in geothermal monitor wells are highly correlated with changes in rainfall pattern. This result

confirms the value of the Wellbore Closure Programme because it shows the behaviour of the aquifers shifted from being dominated by variations in seasonal production to variations in seasonal rainfall.

A simple post-processing model has been developed to represent the behaviour of the surface features of Rotorua. Good or fair matches have been obtained for enthalpy variations (trends and amplitude) for most surface features being monitored as part of the Resource Management Act.

The risk of modification of natural surface manifestations, often important tourist attractions, is frequently pointed out as an issue affecting the public acceptance of geothermal field exploitation. UOA Model 5 represents the first attempt to model individual surface features using a full scale numerical model of the Rotorua geothermal field and to predict the effects of reservoir management on the evolution of surface manifestations. The three dimensional model of the Rotorua geothermal field discussed here offers a tool that can reproduce the system behaviour realistically, essential for assessing the impact of various future production schemes on the geothermal field. Thus model UOA Seasonal should assist with efficient field management, allowing the development and allocation of the resource, while limiting the adverse effects on the surface features of Rotorua.

## Acknowledgment

We thank the Environment Bay of Plenty (EBOP) for providing information on current and past consented geothermal bores as well as temperature versus depth data.

## References

- Arditty, P.C., Ramey, H.J., 1978. Response of a closed well-reservoir system to stress induced by earth tides Society of Petroleum Engineers. 53rd Annual Fall Technical Conference 7484.
- Battistelli, A., Calore, G., Pruess, K., 1997. The simulator TOUGH2/EWASG for modelling geothermal reservoirs with brines and a non condensable gas. Geothermics 26, 437–464.  
<http://monitoring.boprc.govt.nz/MonitoredSites/cgi-bin/hydwebserver.cgi/sites/details?site=238&treetcatchment=26>
- Bluestein, H.B., 1993. Synoptic-Dynamic Meteorology in Midlatitudes II. Oxford University Press.
- Boreham, L., 1985. Rotorua Geothermal Field, the Production and Soak Bores, Databases on dBase II. Oil and Gas Division, Ministry of Energy, Wellington.
- Bradford, E., 1992. Pressure changes in Rotorua geothermal aquifers, 1982–90. Geothermics 21 (1/2), 231–248.
- Cody, A.D., Lumb, J.T., 1992. Changes in thermal activity in the rotorua geothermal field. Geothermics 21 (1/2), 215–230.
- Cody, A.D., 2007. Geodiversity of geothermal fields in the Taupo Volcanic Zone. DOC Res. Dev. 281.
- Environment Bay of Plenty (EBOP), 1999. Rotorua Geothermal Regional Plan. Resource Planning Publication 99/02 ISSN 1170 9022.
- Febrianto, R., Johnson, P., Wong, Y., O'Sullivan, M., O'Sullivan, J., 2013. A computer model of Rotorua geothermal field. In: Proceedings of the 35th New Zealand Geothermal Workshop 2013. Rotorua, New Zealand.
- Giggenbach, W.F., 1995. Variations in the chemical and isotopic composition of fluids

- discharged from the Taupo Volcanic Zone, New Zealand. *J. Volcanol. Geother. Res.* 68 (1), 89–116.
- Gordon, D.A., Scott, B., Mroczek, E.K., 2005. Rotorua Geothermal Field Management Monitoring Update: 2005. Environment Bay of Plenty Environmental Publication 2005/12.
- Graham, D.J., Pearson, S.C.P., Seward, A., O'Halloran, L., 2013. Rotorua Geothermal System: Measurements and Observations July to September 2013. GNS Science Consultancy Report 2013/306. 72.
- Grant, M.A., 1986. The response to exploitation of Rotorua geothermal field. In: Proceedings from the Eleventh Workshop on Geothermal Reservoir Engineering 1986. Stanford University, Stanford, California.
- Heise, W., Caldwell, T.G., Bertrand, E.A., Hill, G.J., Bennie, S.L., Palmer, N.G., 2015. Imaging the deep source of the Rotorua and Waimangu geothermal fields, Taupo volcanic zone, New Zealand. *J. Volcanol. Geotherm. Res.* 314, 39–48.
- Hsieh, P.A., Bredehoeft, J.S., Rojstaczer, S.A., 1988. Response of well aquifer systems to earth tides: problem revisited. *Water Resour. Res.* 24 (3), 468–472.
- Hunt, T.M., 1992. Gravity anomalies, caldera structure, and subsurface geology in the Rotorua area, New Zealand. *Geothermics* 21 (1/2), 65–74.
- Kissling, W., Ellis, S., Charpentier, F., Bibby, H., 2009. Convective flows in a TVZ-like setting with a Brittle/Ductile transition. *Transp. Porous Media* 77 (2), 335–355.
- Kissling, W., 2014. Rotorua Geothermal Bore Water Level Assessment – 2014. GNS Science Consultancy Report 2014/199, 39.
- Leaver, J.D., 2006. Identification and Interpretation of Characteristic Periodic Variations of Near Surface Fluids in the Te roha, Rotorua, and Orakeikorako Geothermal Fields of New Zealand using Wavelet and Fourier Analysis. Thesis submitted in partial fulfilment of the requirements for the degree of Doctor of Philosophy in Mechanical Engineering, The University of Auckland.
- Milicich, S.M., van Dam, A., Rosenberg, M., Rae, A., Bignall, G., 2005. 3-Dimensional geological modelling of geothermal systems in New Zealand – a new visualisation tool. In: Proceedings World Geothermal Congress. Bali, Indonesia.
- Ministry of Energy, 1985. The Rotorua Geothermal Field. A Report of the Geothermal Monitoring Programme and Task Force 1982–1985. Ministry of Energy.
- Mroczek, E.K., Stewart, M.K., Scott, B.J., 2004. Chemistry of the Rotorua Geothermal Field Part 3: Hydrology. Institute of Geological and Nuclear Sciences Client Report 2004/178, 71.
- Narasimhan, T.N., Kanehiro, B.Y., Witherspoon, P.A., 1984. Interpretation of earth tide response of three deep, confined aquifers. *J. Geophys. Res.* 89 (B3), 1913–1924.
- Newson, J., Manninton, W., Sepulveda, F., Lane, R., Pascoe, R., Clearwater, E., O'Sullivan, M.J., 2012. Application of 3d modelling and visualization software to reservoir simulation: leapfrog geothermal and tough2. In: Proceedings Thirty-Seventh Workshop on Geothermal Reservoir Engineering. Stanford University, Stanford, California.
- Nikrou, P., Newson, J., McKibbin, R., 2013. Time series analysis of selected geothermal spring temperature recordings. Waikato Regional Council Technical Report 2013/17.
- O'Shaughnessy, B.W., 2000. Use of economic instruments in management of Rotorua geothermal field, New Zealand. *Geothermics* 29 (4/5), 539–555.
- Pearson-Grant, S.C., Scott, B.J., Mroczek, E.K., Graham, D.J., 2015. Rotorua Surface Feature Monitoring Data Review: 2008–2014. GNS Science Consultancy Report 2015/124, 108.
- Pruess, K., Oldenburg C., Moridis, G., 1999. TOUGH2 User's Guide, Version 2.0, Lawrence Berkeley National Laboratory Report LBNL-43134, Berkeley, CA.
- RGMP, 1985. The Rotorua Geothermal Field: Technical Report of the Geothermal Monitoring Programme 1982–1985. Report to the Ministry of Energy.
- Ratouis, T.M.P., O'Sullivan, M., O'Sullivan, J., 2014. Numerical model of rotorua geothermal field. In: Proceedings Thirty-Ninth Workshop on Geothermal Reservoir Engineering. Stanford University Stanford, California.
- Ratouis, T.M.P., O'Sullivan, M., O'Sullivan, J., 2015. An updated numerical model of rotorua geothermal field. In: Proceedings World Geothermal Congress 2015. Melbourne, Australia.
- Ratouis, T.M.P., O'Sullivan, M.J., O'Sullivan, J.P., 2016a. A numerical model of rotorua geothermal field. *Geothermics* 60, 105–125.
- Ratouis, T.M.P., O'Sullivan, M., O'Sullivan, J., 2016b. Modelling geothermal surface features in the rotorua geothermal field. In: Proceedings 38th New Zealand Geothermal Workshop. Auckland.
- Robert, T., Sirguey, P., Rattenbury, M., Nicolson, J., 2010. Digital rock density map of New Zealand. *Comput. Geosci.* 37 (8), 1181–1191.
- Saptadji, N., O'Sullivan, J., Krzyzosiak, W., O'Sullivan, M., 2016. Numerical modelling of Pohutu geyser, Rotorua, New Zealand. *Geothermics* 64, 401–409.
- Scott, B.J., Cody, A.D., 1997. Effects of bore closure at rotorua, New Zealand. Proceedings NEDO International Geothermal Symposium 1997 270–276.
- Scott, B.J., Gordon, D.A., Cody, A.D., 2005. Recovery of Rotorua geothermal field, New Zealand: progress, issues and consequences. *Geothermics* 34 (2/5), 159–183.
- Soengkono, S., Suhanto, E., Teece, C., Tuah, A.H.A., Mejia Diaz, C.E., Tansupo, K., 2001. Temperature, resistivity and self potential investigations of Kuirau Park, Rotorua geothermal field, New Zealand. In: Proceedings of the 23rd New Zealand Geothermal Workshop. Rotorua, New Zealand.
- Stewart, M.K., Lyon, G.L., Robinson, B.W., Glover, R.B., 1992. Fluid flow in the Rotorua Geothermal Field derived from isotopic and chemical data. *Geothermics* 21 (1/2), 141–163.
- Taylor, C.B., Stewart, M.K., 1987. Hydrology of Rotorua geothermal aquifer, New Zealand. In: Proceedings Int Syrup. Isotope Techniques in Water Resources Development. Vienna. pp. 25–45.
- Weeks, E.P., 1979. Barometric fluctuations in wells tapping deep unconfined aquifers. *Water Resour. Res.* 15 (5), 1167–1176.
- Wood, C.P., 1992. Geology of the Rotorua geothermal system. *Geothermics* 21 (1/2), 25–41.
- Yeh, A., Croucher, A., O'Sullivan, M.J., 2012. Recent developments in the AUTOUGH2 simulator. In: Proceedings TOUGH Symposium 2012. Berkeley, California.